Dear Author,

Please use this PDF proof to check the layout of your article. If you would like any changes to be made to the layout, you can leave instructions in the online proofing interface.

Making your changes directly in the online proofing interface is the quickest, easiest way to correct and submit your proof. Please note that changes made to the article in the online proofing interface will be added to the article before publication, but are not reflected in this PDF proof.

If you would prefer to submit your corrections by annotating the PDF proof, please download and submit an annotatable PDF proof by following this link:

https://rscweb.proofcentral.com/en/offline.html?token=2c01f18dda6aafa42ba481b492b13307

Environmental Science: Processes & Impacts c9em00599d

We have presented the graphical abstract image and text for your article below. This briefly summarises your work, and will be presented with your article online.

PAPER

1

Natural and anthropogenic sources of bromoform and dibromomethane in the oceanographic and biogeochemical regime of the subtropical North East Atlantic

Melina Mehlmann, Birgit Quack, Elliot Atlas, Helmke Hepach and Susann Tegtmeier

Transport of air masses from the subtropics, enriched in trace gases from the oceans, coasts and islands, towards lower latitudes under the trade inversion and uplift to the stratosphere in tropical deep convection.

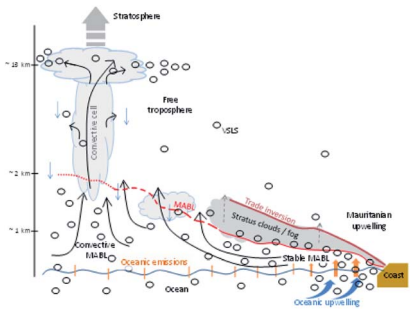

Please check this proof carefully. Our staff will not read it in detail after you have returned it.

Please send your corrections either as a copy of the proof PDF with electronic notes attached or as a list of corrections. **Do not edit the text within the PDF or send a revised manuscript** as we will not be able to apply your corrections. Corrections at this stage should be minor and not involve extensive changes.

Proof corrections must be returned as a single set of corrections, approved by all co-authors. No further corrections can be made after you have submitted your proof corrections as we will publish your article online as soon as possible after they are received.

Please ensure that:

- The spelling and format of all author names and affiliations are checked carefully. You can check how we have identified the authors' first and last names in the researcher information table on the next page. **Names will be indexed and cited as shown on the proof, so these must be correct.**
- Any funding bodies have been acknowledged appropriately and included both in the paper and in the funder information table on the next page.
- All of the editor's queries are answered.
- Any necessary attachments, such as updated images or ESI files, are provided.

Translation errors can occur during conversion to typesetting systems so you need to read the whole proof. In particular please check tables, equations, numerical data, figures and graphics, and references carefully.

Please return your **final** corrections, where possible within **48 hours** of receipt following the instructions in the proof notification email. If you require more time, please notify us by email to espi@rsc.org.

Funding information

Providing accurate funding information will enable us to help you comply with your funders' reporting mandates. Clear acknowledgement of funder support is an important consideration in funding evaluation and can increase your chances of securing funding in the future.

We work closely with Crossref to make your research discoverable through the Funding Data search tool (http://search.crossref.org/funding). Funding Data provides a reliable way to track the impact of the work that funders support. Accurate funder information will also help us (i) identify articles that are mandated to be deposited in **PubMed Central (PMC)** and deposit these on your behalf, and (ii) identify articles funded as part of the **CHORUS** initiative and display the Accepted Manuscript on our web site after an embargo period of 12 months.

Further information can be found on our webpage (http://rsc.li/funding-info).

What we do with funding information

We have combined the information you gave us on submission with the information in your acknowledgements. This will help ensure the funding information is as complete as possible and matches funders listed in the Crossref Funder Registry.

If a funding organisation you included in your acknowledgements or on submission of your article is not currently listed in the registry it will not appear in the table on this page. We can only deposit data if funders are already listed in the Crossref Funder Registry, but we will pass all funding information on to Crossref so that additional funders can be included in future.

Please check your funding information

The table below contains the information we will share with Crossref so that your article can be found *via* the Funding Data search tool. **Please check that the funder names and grant numbers in the table are correct and indicate if any changes are necessary to the Acknowledgements text.**

Funder name	Funder's main country of origin	Funder ID (for RSC use only)	Award/grant number
Deutsche Forschungsgemeinschaft	Germany	501100001659	TE1134
GEOMAR Helmholtz-Zentrum für Ozeanforschung Kiel	Germany	501100003153	EP533
National Aeronautics and Space Administration	United States	100000104	NNX17AE43G

Researcher information

Please check that the researcher information in the table below is correct, including the spelling and formatting of all author names, and that the authors' first, middle and last names have been correctly identified. **Names will be indexed and cited as shown on the proof, so these must be correct.**

If any authors have ORCID or ResearcherID details that are not listed below, please provide these with your proof corrections. Please ensure that the ORCID and ResearcherID details listed below have been assigned to the correct author. Authors should have their own unique ORCID iD and should not use another researcher's, as errors will delay publication.

Please also update your account on our online manuscript submission system to add your ORCID details, which will then be automatically included in all future submissions. See here for step-by-step instructions and more information on author identifiers.

First (given) and middle name(s)	Last (family) name(s)	ResearcherID	ORCID iD
Melina	Mehlmann		
Birgit	Quack		0000-0003-4123-5845

Elliot	Atlas		0000-0003-3847-5346
Helmke	Hepach		
Susann	Tegtmeier		

Queries for the attention of the authors

Journal: **Environmental Science Processes & Impacts**

Paper: **c9em00599d**

Title: **Natural and anthropogenic sources of bromoform and dibromomethane in the oceanographic and biogeochemical regime of the subtropical North East Atlantic**

For your information: You can cite this article before you receive notification of the page numbers by using the following format: (authors), Environ. Sci.: Processes Impacts, (year), DOI: 10.1039/c9em00599d.

Editor's queries are marked on your proof like this **1**, **2**, etc. and for your convenience line numbers are indicated like this 5, 10, 15, ...

Please ensure that all queries are answered when returning your proof corrections so that publication of your article is not delayed.

Query Reference	Query	Remarks
1	Have all of the author names been spelled and formatted correctly? Names will be indexed and cited as shown on the proof, so these must be correct. No late corrections can be made. Please tick this box or indicate your confirmation if you have no corrections to make to the proof ☐	
2	Do you wish to indicate the corresponding author(s)? If so, please specify the corresponding author(s).	
3	Do you wish to add an e-mail address for the corresponding author? If so, please provide the relevant information.	
4	The brackets appear to be unpaired in the sentence beginning "Temperature–Salinity (TS)...". Please check and indicate any changes that are required.	
5	Please note that a conflict of interest statement is required for all manuscripts. Please read our policy on Conflicts of interest (http://rsc.li/conflicts) and provide a statement with your proof corrections. If no conflicts exist, please state that "There are no conflicts to declare".	
6	Have all of the funders of your work been fully and accurately acknowledged? Please tick this box or indicate your confirmation if you have no corrections to make to the proof ☐	
7	Ref. 20: Please provide the page (or article) number(s).	
8	Ref. 41: Please provide the page (or article) number(s).	
9	Ref. 49: Please provide the journal title and page (or article) number(s).	
10	Ref. 55: Please provide the page (or article) number(s).	
11	Ref. 87: Please provide the page (or article) number(s).	

12	Ref. 89: Please provide the page (or article) number(s).	
13	Please check that "Fig. 15" has been displayed correctly.	

Environmental Science Processes & Impacts

ROYAL SOCIETY OF CHEMISTRY

PAPER

Natural and anthropogenic sources of bromoform and dibromomethane in the oceanographic and biogeochemical regime of the subtropical North East Atlantic

Melina Mehlmann,[a] Birgit Quack, [a] Elliot Atlas, [b] Helmke Hepach[a] and Susann Tegtmeier[c]

Cite this: DOI: 10.1039/c9em00599d

Received 21st December 2019
Accepted 21st February 2020

DOI: 10.1039/c9em00599d

rsc.li/espi

The organic bromine compounds bromoform ($CHBr_3$) and dibromomethane (CH_2Br_2) influence tropospheric chemistry and stratospheric ozone depletion. Their atmospheric abundance is generally related to a common marine source, which is not well characterized. A cruise between the three Macaroenesian Archipelagos of Cape Verde, the Canaries and Madeira revealed that anthropogenic sources increased oceanic $CHBr_3$ emissions significantly close to some islands, especially at the Canaries, while heterotrophic processes in the ocean increased the flux of CH_2Br_2 from the sea to the atmosphere in the Cape Verde region. As anthropogenic disinfection processes, which release $CHBr_3$ in coastal areas increase, and as more CH_2Br_2 may be produced from increased heterotrophy in a warming, deoxygenated ocean, both sources could supply higher fractions of stratospheric bromine in the future, with yet unknown consequences for stratospheric ozone.

Environmental significance

Bromoform ($CHBr_3$) and dibromomethane (CH_2Br_2) are important bromine sources to both the troposphere and the lower stratosphere. Their sources in the Subtropical North Atlantic have mainly been attributed to natural processes. This paper tries to identify the additional impact of anthropogenic sources and quantifies the air–sea fluxes of both compounds around the Macaronesian Archipelagos of the Cape Verdes, the Canaries and Madeira. The organobromine gases from locally increased fluxes are transported by the trade winds from their source regions in the extra tropics towards the equator, where deep convection can transport them to the stratosphere. The data give new insights into important oceanographic and biogeochemical cycles in the Subtropical North Atlantic and how they are impacted by anthropogenic activities.

1 Introduction

Human emissions of pollutants and greenhouse gases into the atmosphere alter air quality and climate.[1,2] While the most commonly discussed change is increased CO_2 concentration, there is a wide range of other chemically and radiatively active trace gases that are subject to change. Many of these gases have short atmospheric lifetimes and, hence, regional impacts, but their influence may lead to global consequences. The oceans contribute significantly to the global emissions of short-lived, climate-active gases, which include halogenated volatile organic compounds such as bromoform ($CHBr_3$) and dibromomethane (CH_2Br_2). Both gases play a critical role in tropospheric ozone chemistry, photooxidant cycling (which controls the atmosphere's ability to rid itself of pollutants), and stratospheric ozone loss.[3,4] Ocean surface processes can exert a critical control on the fluxes of these gases to and from the atmosphere, thus impacting climate and atmospheric chemistry regionally and globally.

Tropical processes are of special importance for the changing chemistry and composition of the stratosphere. Stratospheric ozone is mainly created in the tropical lower stratosphere and transported upwards and towards the winter pole by large-scale atmospheric circulation. Most long-lived and short-lived trace gases in tropospheric air enter the stratosphere in the tropics and follow the same transport pathways.[5] In subtropical regions, marine air under the trade wind inversion can be transported by the trade winds horizontally near the surface over long distances towards the equator with almost no vertical exchange until it reaches areas of deep convection, which rapidly deliver boundary layer air to the upper troposphere and, eventually, to the stratosphere.[6] While anthropogenic long-lived chlorine and bromine trace gases dominate

[a]Chemical Oceanography, GEOMAR Helmholtz Centre for Ocean Research Kiel, Kiel, Germany
[b]Department of Atmospheric Sciences, RSMAS, University of Miami, Miami, Florida, USA
[c]Institute of Space and Atmospheric Studies, University of Saskatchewan, Saskatoon, Canada

stratospheric ozone loss processes, marine emissions of halogenated very short-lived substances (VSLS) such as $CHBr_3$ and CH_2Br_2, are also of increasing concern.[7–12]

A global, so called bottom-up, emission climatology ($1° \times 1°$) of $CHBr_3$ and CH_2Br_2, derived from observations by Ziska *et al.*,[13] attributed 70% of the global $CHBr_3$ emissions to coastal regions. Observed tropospheric concentrations in remote locations show a good agreement with this VSLS emission climatology.[14,15] Compared to model-derived top-down estimates, however, the emission climatology is lower and localized sources were suggested as a cause for the mismatch.[13] In addition, coastlines are difficult to resolve in global models and the coastal data are very sparse.[16] Recent progress has been made in the bottom-up oceanic emission inventories for $CHBr_3$ and CH_2Br_2, powered by a data-oriented machine-learning emulator, which includes a representation of ocean biogeochemistry control.[17] Overall, the observed mean surface atmospheric concentrations, as well as the seasonal and spatial variations of $CHBr_3$ and CH_2Br_2, are reasonably captured by the new model framework. Still the underlying production processes and sources of the compounds remain unclear, which may cause uncertainties in the future predictions of the oceanic emissions.

$CHBr_3$ and CH_2Br_2 are released naturally from macroalgae and phytoplankton. While phytoplankton and macroalgae are known to produce many halogenated compounds, $CHBr_3$ is generally the dominant product.[9] Its production is related to the haloform reaction, which produces polyhalogenated methanes from organic compounds and seawater halides, following their oxidation to hypo-halides by enzymes.[18] $CHBr_3$ sometimes shows correlations with fucoxanthin, a marker pigment for diatoms,[19,20] while also correlations to haptophytes and cyanobacteria have been observed.[21,22] Nanomolar concentrations of $CHBr_3$ detected in the vicinity of macroalgal beds are a possible result of defense mechanisms in the algae, which produce and emit variable $CHBr_3$ levels due to stress, which is also related to light.[23]

Less is known about the sources of CH_2Br_2. Its co-occurrence with $CHBr_3$ has been widely reported. Common marine sources, with a ten times higher production of $CHBr_3$ from macroalgae, have been reported.[24] On the other hand, bromination of dissolved organic matter (DOM), which represents an extracellular formation process of brominated halocarbons from marine algae, has, only produced $CHBr_3$ in artificial seawater.[25] The study of Lin and Manley[26] in natural seawater indicates that at least a small amount of CH_2Br_2 could result from this process, which suggests that the composition of bromocarbons produced from the halogenation of DOM is highly substrate-dependent. Towards the open ocean, the ratio between $CHBr_3$ and CH_2Br_2 declines in the surface ocean, either due to a faster photolysis of $CHBr_3$ compared to CH_2Br_2,[23] or to a lower $CHBr_3$ to CH_2Br_2 production ratio in the open ocean. An increase of CH_2Br_2 concentrations with depth has been observed in the Mauritanian upwelling.[27] $CHBr_3$ could be converted to CH_2Br_2 *via* reductive hydrogenolysis[28] under less oxic conditions or *via* microbial reduction in the thermocline waters. Microbial reduction was subject of recent laboratory-based incubation studies using stable isotopes of $CHBr_3$ and CH_2Br_2. In one of the first studies, involving stable isotopes of brominated halocarbons in marine waters[29] a loss of $^{13}CHBr_3$ was followed by the appearance of $^{13}CH_2Br_2$. Clear evidence for the bacterial formation of $^{13}CH_2Br_2$ from $^{13}CHBr_3$ was also found in incubation studies, which involved bacterial strains from temperate and subarctic marine waters.[30,31] The studies indicate that the production of CH_2Br_2 from heterotrophic cycling of $CHBr_3$ is a widespread phenomenon in the marine environment. The subsequent entrainment of thermocline waters into the mixed layer could contribute to the ratio shift in the open ocean and upwelled waters. Furthermore, $CHBr_3$ may be lost faster from surface waters over time as it has a greater sea-air concentration gradient compared to CH_2Br_2 towards the open ocean.[20,27]

$CHBr_3$ is found in micromolar concentrations in disinfected seawater, as in cooling waters from coastal power plants[32] and desalination plants[33] as well as in treated ballast water[11] and industrialized urban environments.[34] Production of brominated halocarbons in seawater is thought to result from similar reactions as the natural formation of brominated halocarbons.[25,26] The presence of high concentrations of bromine ions in seawater leads to increased production of brominated halocarbons in comparison to disinfection of fresh water. The trihalomethanes formed during chlorination of seawater are 96–98% comprised of $CHBr_3$.[35] The composition of dissolved organic matter present in seawater seems to strongly favor the production of trihalomethanes (THM) such as $CHBr_3$.[32] $CHBr_3$ is generally the most abundant halogenated organic compound resulting from disinfection of seawater in the environment.[34,36] Other disinfection by-products (DBP) in the effluents, as halogenated phenols, can lead to unfavourable effects on the environment and on human health.[34,37] $CHBr_3$ shows highly elevated concentrations in coastal urbanized and industrialized regions, which may represent an important and increasing contribution to the global ocean emission budget of bromocarbons. Many industrial processes at coastlines use disinfected seawater for cooling purposes,[34] which entail an increase in the marine concentrations and emissions of $CHBr_3$ upon their discharge.[7,11]

While atmospheric $CHBr_3$ mixing ratios over the open oceans and around the Cape Verde Atmospheric Observatory (CVAO) are generally around 0.5–1 pptv,[38,39] episodic increases to >40 pptv there on summer days,[40] and elevated abundances of >15 pptv in the Mauritanian upwelling region during several cruises have also been observed.[21,27,41,42] The high mixing ratios of $CHBr_3$ and other trace gases over the upwelling were associated to their accumulation in shallow marine boundary layers. The sources for the elevated concentrations at the coastal CVAO remain speculative and include local seaweed.[40]

First studies of reactive volatile halogenated compounds, including $CHBr_3$ and CH_2Br_2, in the Macaronesian Archipelagos were conducted a few decades ago by Class and Ballschmiter,[43–45] Frank *et al.*[46] and Fischer *et al.*[47] The early measurements revealed atmospheric $CHBr_3$ of 20–460 pptv over beaches of the islands Tenerife and the Azores and up to 26 000 pptv were also measured directly over an isolated rock pool on Gran Canaria,[48] indicating macroalgae to be the most likely cause of these high concentrations. These are the highest

atmospheric mixing ratios ever recorded, and historically $CHBr_3$ has always been seen as a biogenic marine marker in air.[21] During a few recent measurements in arbitrarily picked coastal sampling locations Quack *et al.*[49] found extraordinarily high concentrations of >10 nmol L^{-1} in seawater at beaches in the south and north-east of Tenerife, with no visible macroflora around, but with possible anthropogenic input. The identification of the relevant sources remains an open research task. Quantifying their spread into the open ocean and their contribution to the atmospheric boundary layer requires multidisciplinary efforts combining oceanic, atmospheric, biological and modeling studies.

The research cruise POS533 with the RV Poseidon into the Subtropical North East Atlantic investigated the $CHBr_3$ and CH_2Br_2 distribution in ocean and atmosphere, together with physical, biogeochemical and biological parameters, around the islands of Madeira, Tenerife, Gran Canary and the Cape Verde Archipelago. The cruise transected mainly downwind (leeward) of the islands to investigate the islands influence on ocean and atmosphere, while also the windward sides of the anthropogenic influenced regions was investigated. The southern islands of the Macaronesian Archipelago provide the ideal region to study the various sources of $CHBr_3$ and CH_2Br_2, as the region comprises different marine environments and the islands have anthropogenic sources, such as power stations, desalination plants and recreational water outflow. The dynamic coupling between ocean and atmosphere and the environmental differences between the islands were taken into account for characterizing oceanic sources and air–sea fluxes of both compounds for the differently populated islands of the southern Macaronesian region.

2 Data and methods

2.1 Cruise overview

Data for this study were collected on board the RV Poseidon research vessel during the POS533 cruise. The cruise started on 28th of February 2019 in Mindelo on Sao Vicente (Cape Verde), and crossed nearby the archipelagos islands Santo Antao, Sao Nicolau, Fogo, Santiago, Boavista and Sal. Five days of transit against the northeastern trade winds towards the Canaries was followed by a transect through the coastal waters of Hierro, La Gomera, Tenerife, and Gran Canary. After a stopover in Las Palmas (Gran Canary) the ship sailed northwards, carried out two transects leeward of Madeira, made a stop in Funchal, where the sampling ended and the cruise ended in Las Palmas on the 22nd of March 2019 (Fig. 1).

Sampling was divided into underway and depth sampling. Underway seawater samples were collected from the continuously flowing by-pass of a ship mounted high volume (~100 L h^{-1}) pump, which was deployed in the hydrographic shaft in the ships moon pool at around 6 m depth. The high volume throughput avoids contamination, provides real time supply of the seawater beneath the moving ship and feeds several automated instruments. Air samples were taken from the compass deck at a height of 13.7 m with a metal bellows pump and were stored in stainless

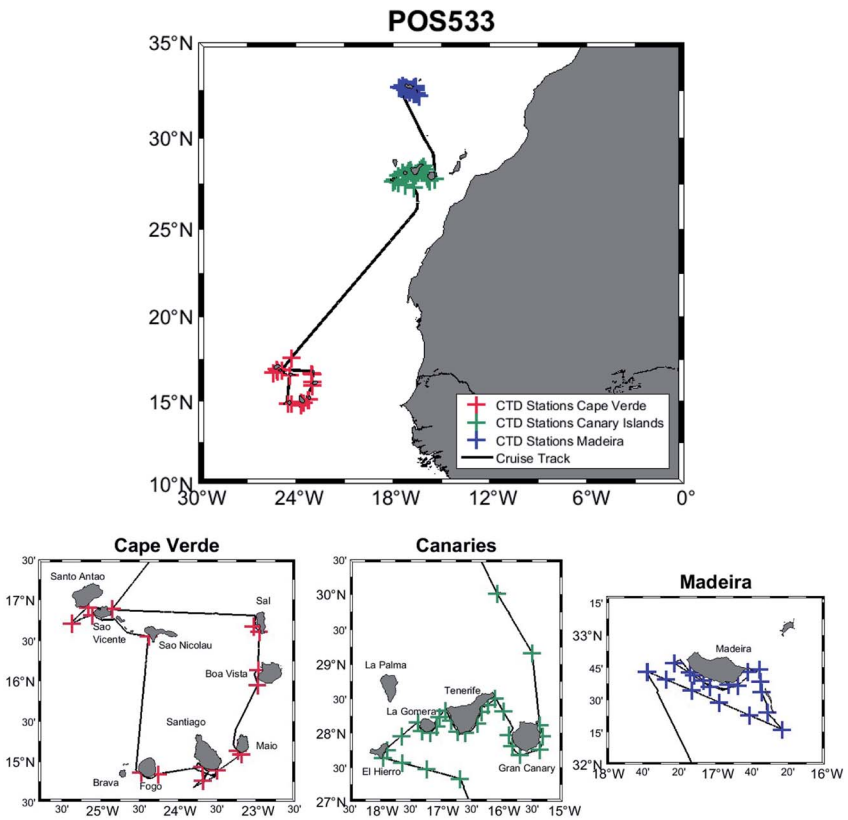

Fig. 1 POS533 cruise track (black line) with CTD station locations marked by crosses.

steel canisters. The ships track was chosen, so that the track was mainly against the predominant northeastern trade wind direction, to avoid contamination by the ships stack. Conductivity, temperature, and depth (CTD) measurements were taken from 69 stations, ranging from the surface to 100 m depth for shallow stations and 4000 m for deep stations. A bottle rosette sampler was operated with the CTD, containing twelve 10 L Niskin bottles for seawater sampling and additional sensors for depth, pressure, salinity, temperature, dissolved oxygen, sound speed and fluorescence. CTD fluorescence is given in an arbitrary unit that is approximately equal to μg L^{-1} chlorophyll (data are not calibrated). CTD pressure data were used for depth measurements. Oxygen was calibrated using the Winkler Titration method. During the cruise, standard underway oceanic parameters as salinity, temperature, oxygen, and fluorescence were recorded by onboard instrumentation (thermosalinograph: SeaCat SBE18 and SBE21, fluorometer: Wetlabs ECO FLRT). Underway fluorescence was recorded as chlorophyll data in μg L^{-1}, but is also not calibrated. Weather data including wind measurements were collected by an on-board weather station in cooperation with the DWD (Deutscher Wetterdienst – German weather service). Continuous underway data are available through the DSHIP platform (http://dship-poseidon.geomar.de). All sampling data are available on the GEOMAR (https://portal.geomar.de/group/aimac/home).

2.2 Halocarbon analysis and air–sea flux calculations

Sampling of the halocarbons $CHBr_3$ and CH_2Br_2 in seawater was done with 250 mL amber glass bottles from the CTD-rosette bottles and from the underway supply in three-hour intervals, which were filled bubble free and closed with Teflon lids. The samples were stored in a ~7 °C refrigerator until they were measured with a purge and trap system attached to a gas chromatograph (Agilent 6890N) with mass spectrometric detection (Agilent Technologies 5975 inert XL MSD) (GC-MS), within 12 hours after the sampling. Prior to analysis, the samples were warmed to room temperature (~20 °C) to ensure purge efficiency and consistency. The bottles were attached to a manifold, which pressurizes the top of the sample with helium and fills the purge-chamber with 30 mL of the seawater through a second submerged outlet, so that a pure sample can by transferred. $CHBr_3$ and CH_2Br_2 concentrations were measured by purging 30 mL of sample water at 70 °C in a long glass chamber for 45 min with a stream of helium at around 50 mL min^{-1}, resulting in a purge efficiency of ~98%.[21] A Nafion dryer (Ansyco GmbH, TT-050) was installed for the desiccation of the purge flow, using a counter-flow of 100 mL min^{-1} of N_2. The volatilized trace gases were trapped between −150 and −170 °C above liquid nitrogen in a coil of deactivated stainless steel tubing. After purging, the compounds were desorbed from the trap and injected into the GC-MS by heating the trap electronically to 180 °C for 1.5 min. The sample was then separated on a 60 m by 0.25 mm Rtx-VGC capillary column (film thickness = 1.4 μm) and finally detected by the MS in single ion mode. The concentrations were quantified with external standards, which were volumetrically prepared in methanol. The calibration curves were prepared with 1–4 μL of standards containing 0.02, 0.3 and 3 pmol of compound per μL. Calibration curves were run in triplicate for sample quantitation.[21] The R^2-values of the calibration curves are 0.99, while the seawater measurements generally have a reproducibility of <5% for CH_2Br_2 and <10% for $CHBr_3$.

Underway air samples of POS533 were analyzed for halocarbons at the Rosenstiel School of Marine and Atmospheric Sciences (RSMAS) in Miami using GC/MS. The samples were mostly taken simultaneously with underway seawater samples. Few air measurements, taken with a delay to the corresponding water samples, were manually assigned to the anticipated sample location to generate air and water sample pairs for comparison and flux calculation purposes. If the delay was more than three hours, an average value between the previous and following sample was calculated.

Air–sea fluxes of CH_2Br_2 and $CHBr_3$ were calculated using the Nightingale *et al.*[50] air–sea exchange parameterization and the adjustments proposed in Quack and Wallace[51] and Hepach *et al.*[21] Compound specific transfer coefficients (kw) were derived from the transfer coefficient k_{CO_2} of CO_2 by Schmidt number corrections (Sc) as described in Quack and Wallace.[51] A positive air–sea flux describes a supersaturation of the compounds in the ocean and therewith an emission form the ocean to the atmosphere and is termed sea–air flux in the manuscript.

3 Oceanic and atmospheric environment of the Macaronesian region during POS533

3.1 Oceanic currents and water masses

The general circulation pattern in the subtropical North East Atlantic includes several central water currents (Fig. 2), which

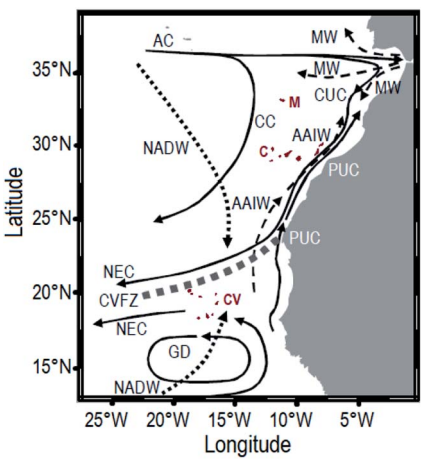

Fig. 2 The subtropical North East Atlantic with main circulation features in central (continuous lines), intermediate (dashed lines) and deep (dotted lines) waters. AC: Azores Current, CUC: Canary Upwelling Current, CC: Canary Current, PUC: Poleward Undercurrent, NEC: North Equatorial Current, GD: Guinea Dome, MW: Mediterranean Water, AAIW: Antarctic Intermediate Water, NADW: North Atlantic Deep Water, CVFZ: Cape Verde Frontal Zone.[53] In red: CV: Cape Verde, C: Canaries, M: Madeira.

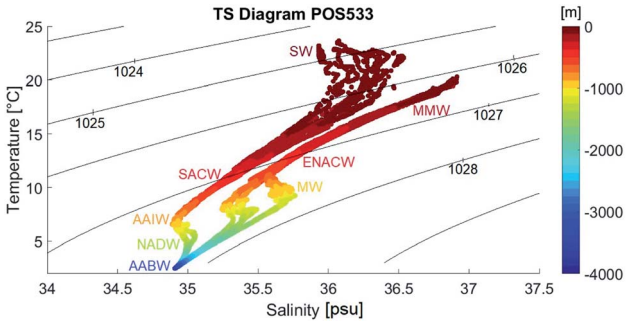

Fig. 3 Temperature–Salinity (TS) diagrams from POS533 Color coding indicates depth). SW: Surface Waters, MMW: Madeira Mode Water, ENACW: Eastern North Atlantic Central Water, SACW: South Atlantic Central Water, MW: Mediterranean Water, AAIW: Antarctic Intermediate Water, NADW: North Atlantic Deep Water, AABW: Antarctic Bottom Water.

carry upper ocean water masses with fairly linear temperature-salinity relations.[52] At intermediate depths Antarctic Intermediate Waters flows north along the West African coast, while at the Mediterranean Throughflow, Mediterranean Water enters the Atlantic basin and transports salty waters south. Deepwater masses in the region are North Atlantic Deep Water, containing a salinity maximum and Antarctic Bottom water.[52] All water masses where encountered during POS533 (Fig. 3).

The Temperature–Salinity (TS) relation of the POS533 CTD samples separates the Cape Verde Islands, the Canaries and Madeira (Fig. 3). The central water masses for the Cape Verde stations were South Atlantic Central Water (SACW) with salinities of 34.3–35.8 psu. Canary Islands and Madeiran TS curves identified Eastern North Atlantic Central Water (ENACW) with more saline waters, above Mediterranean Water (MW) with high salinities reaching from 35.3–35.7 psu and temperatures of 4.0–8.0 °C. Surface waters around Madeira included Madeira Mode Water (MMW) with 16.0–18.0 °C and salinities of 36.5–36.8 psu.[54]

3.2 Temperature, salinity, oxygen and fluorescence in the water column

Distinctive differences of the mean seawater properties existed for three island groups (Fig. 4 and 17–23 in the Appendix). Surface temperatures were highest at Cape Verde (22–23 °C), followed by the Canaries (19.0 °C) and Madeira (18.0 °C). In the ocean interior, the mean temperature profile for Cape Verde (red) was lowest and the Madeira (blue) mean interior temperature was highest. While Cape Verde mean temperature homogeneously decreased with depth, Canaries (green) and Madeira mean temperatures exhibited a change in temperature

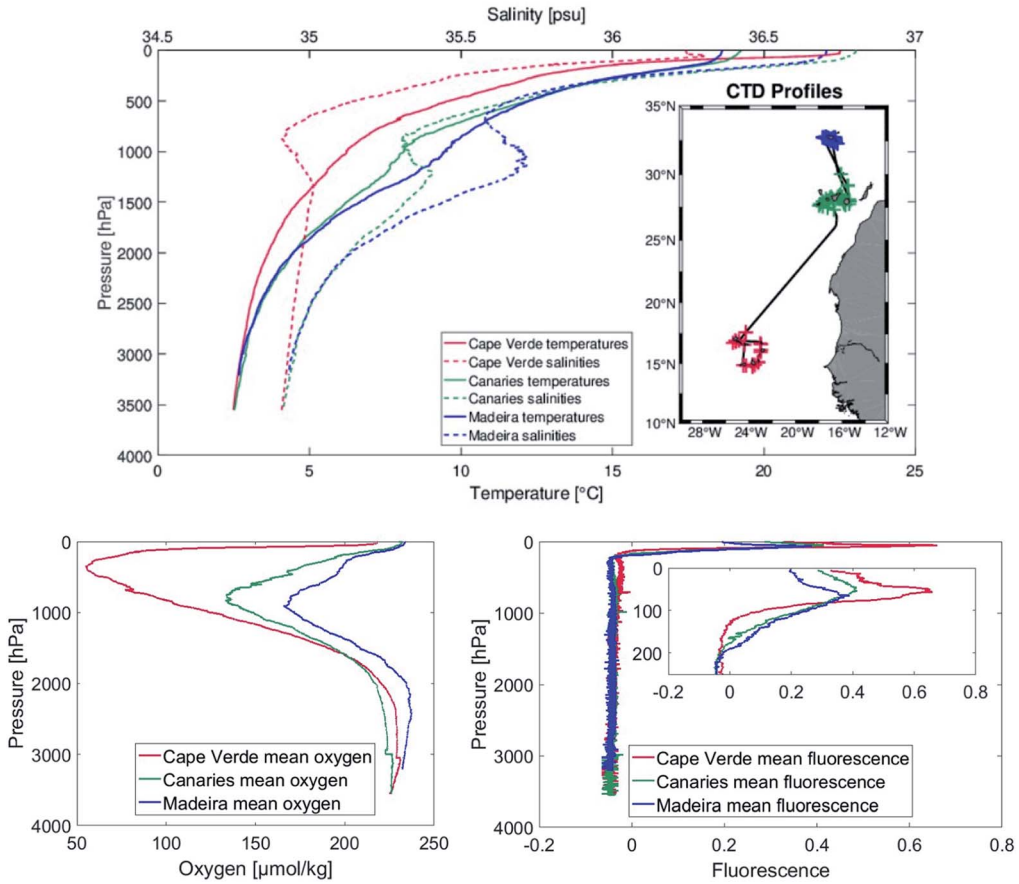

Fig. 4 Mean temperature, salinity, fluorescence, and oxygen profiles. Cape Verde CTD stations: red, Canary Islands CTD stations: green, Madeira CTD stations: blue.

decrease at around 1000 m depth, where Mediterranean water (MW) is located.

The Cape Verde mean salinity was lower (SACW) than salinity around the Canary Islands and Madeira (higher saline ENACW) in the upper 1000 m. The highest salinities were found in the Canary surface waters (Fig. 17 in the Appendix).

The subtropical East Atlantic is known for an extended horizontal Oxygen Minimum Zone (OMZ) with oxygen minima below 80 down to 40 μmol kg^{-1} east of the Cape Verde Islands and at a water column depth of around 200 m.[55] The oxygen profiles during POS533 showed a decrease from the surface to around 400 m depth for Cape Verde, and a decrease to 900 m depth for the Canaries and Madeira (Fig. 4 and 18 in the Appendix). Cape Verde oxygen decreased down to under 60 μmol kg^{-1}, while the minima around the Canary Islands and Madeira reached 140 and 160 μmol kg^{-1}.

Subsurface fluorescence maxima were found in all three archipelagos (Fig. 4 and 19 in the Appendix). The highest fluorescence was found at Cape Verde at around 50 m depth, valuing 0.7. Canary Islands fluorescence maximum was at around 40 m depth and reached 0.4 and Madeira had a fluorescence maximum at around 60 m depth of below 0.4. Below 200–250 m fluorescence was zero for all profiles.

The Mixed Layer Depths (MLDs) during POS533 varied between the islands (Fig. 20 in the Appendix) and generally reflected a deep winter situation, where higher winds lead to stronger mixing. The shallowest mean MLD was found for the southernmost Cape Verde islands with 41.6 m (range: 28.2–66.0 m), followed by a mean MLD at the Canary Islands of 70 m (range: 26.0–166.9 m) and the deepest mean MLD was found at Madeira of 94.3 m (range: 33.8–182.0 m).

Due to the northeastern trade winds, cold nutrient rich central waters are upwelled along the western coast of Africa. The upwelling is a formation region of nutrient rich, cold core, anticyclonic mode water eddies[56] and other cyclonic and anticyclonic eddies. The frequent occurrence of eddies in the region play, together with upwelling filaments, an important role in the lateral mixing and transport of physical and biogeochemical properties and, thereby, they modulate biogeochemistry and biological productivity.[57–61] The dynamic region leads to different properties between the stations and especially between the underway samples.

3.3 Sea surface temperature (SST), salinity (SSS) and fluorescence along the cruise track

Sea surface temperatures reached up to 24.0 °C at the most southern islands. Temperatures decreased towards the north throughout the entire cruise. Around the northern Cape Verde islands, surface temperatures were near 22.0 °C (Fig. 5, top right). Fluorescence, and therefore chlorophyll α, was highest at Cape Verde with higher values in the east compared to the west.

Surface salinity values around Cape Verde were the lowest throughout the cruise, with values reaching from 36.0–36.4 psu (Fig. 5, top left). Salinity was highest at the Canaries, especially around the coasts of El Hierro and La Gomera.

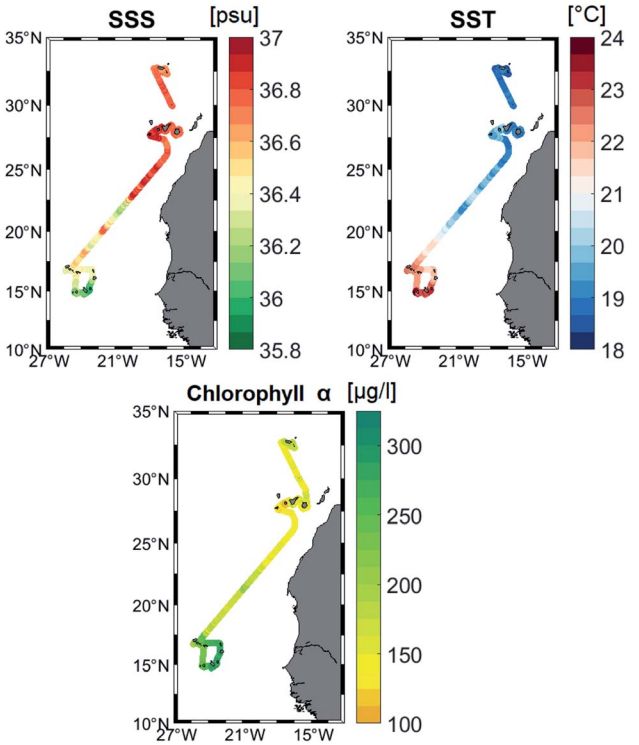

Fig. 5 Underway surface parameters along the POS533 cruise track. Top left: sea surface salinity (SSS), top right: sea surface temperature (SST), bottom: chlorophyll α.

Maxima reached here close to 37.0 psu. Generally, a weak zonal gradient was observed with lower salinities in the east compared to the west. A similar temperature gradient reached from nearly 20.0 °C at El Hierro to 18.2 °C along the coast of Gran Canary (Fig. 5, top right). For chlorophyll α, the zonal gradient of the overall low values was opposite to that of temperature and salinity. Fluorescence and chlorophyll α were locally much more variable than temperature and salinity. Madeira showed minimum temperatures down to 18.0 °C, medium salinities of around 36.7 psu and low chlorophyll α as well.

The islands act as a physical barrier, blocking both wind and ocean current. This leads to a windward side and a sheltered leeward side for each island with accelerated winds in between. The trade winds interaction with the islands develops strong turbulent effects in the lower layers of the atmosphere, which feeds back to the ocean surface.[62–64] Conversely, ocean features generated by islands, such as mesoscale eddies, filaments and warm wakes, generally generate distinct SST signatures,[59] which in return feed back to the overlaying atmosphere.[65]

The difference between surface air and sea surface temperatures during POS533 (Fig. 6) reveals some of the interaction between atmosphere, ocean and the islands. Negative values (blue) illustrate higher air temperatures than ocean temperatures and therefore suggest a stable stratification. If the ocean surface temperature is larger than above air temperatures, a positive value (red) indicates unstable stratification and a heat flux from the sea to the lower atmosphere.

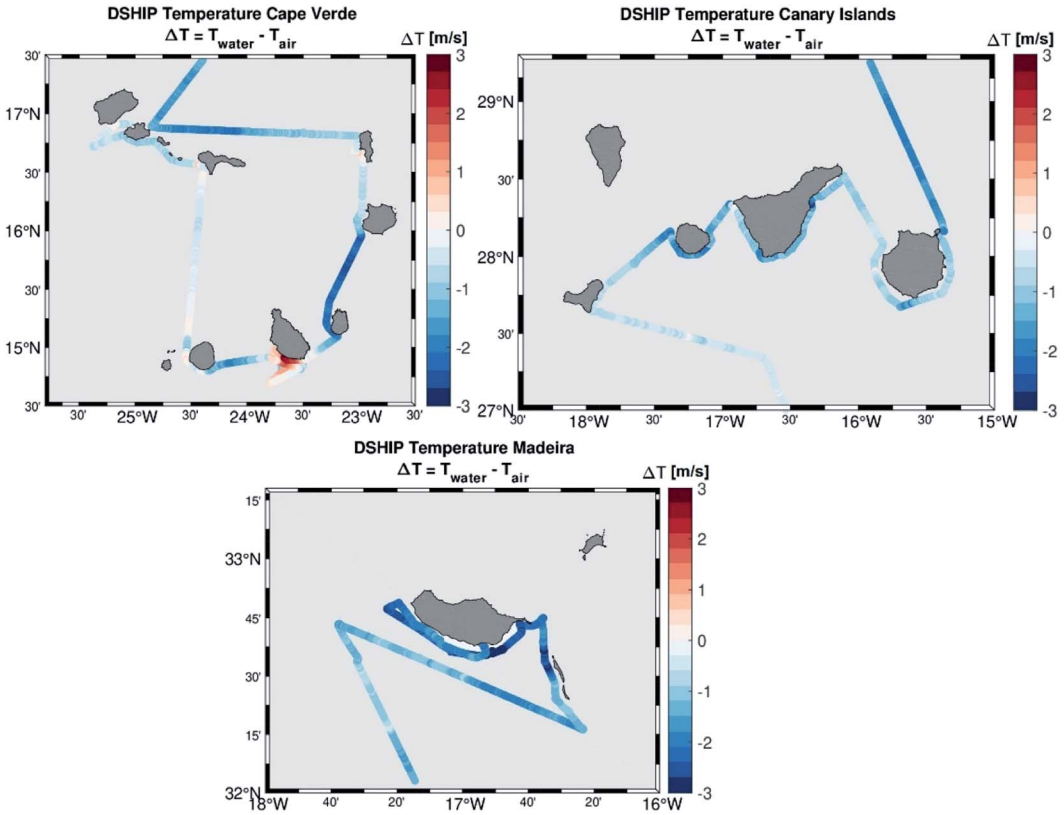

Fig. 6 Difference between sea surface temperature and surface air temperature ($T_{water} - T_{air}$).

3.4 Atmospheric environment in the Macaronesian region during POS533

The region of the Macaronesian islands is dominated by the northeastern trade winds under the stable trade inversion, which limits turbulent mixing and is generally stronger during daytime and in summer. Due to the quite zonal distribution of the Cap Verdes and the Canaries, northeastern coasts are windward and southwestern coasts are leeward of the trade winds. Madeira's coasts can similarly be divided into the northern coast facing the prevailing wind and the southern leeward coasts (Fig. 7).

The average wind speed during POS533 was high with 9.8 m s^{-1}. In general, wind speeds at Cape Verde were close to average, and only peaked around the southern tip of Santo Antao (20.0 m s^{-1}) and at the southern coast of Santiago (25.5 m s^{-1}). Around the Canaries, stronger winds were observed on the eastern and weaker wind speeds on the western coasts. Wind speed varied between 1.0 and 21.6 m s^{-1}. Around Madeira average wind speed was highest with 15.0 m s^{-1}, with maximum wind speeds reaching 22.3 m s^{-1} at the southeastern side of the island (Fig. 7).

Around the islands, cooler water masses and warm marine mesoscale anomalies have been observed to create thermal inversions in concert with the synoptic conditions (Fig. 6). These interactions entail boundary layers between 300 to 1500 m height over the timescale of days interacting with the trade inversion.[62,64,66] This has a significant influence on the boundary layer concentrations of trace gases emitted in the coastal ocean and on their air–sea exchange.

While the trade winds generally facilitate the dispersion of primary pollutants at the islands coastal environments, the local winds, characterized by typical daily sea-land breezes, create positive feedbacks that emphasize air pollution episodes.[62] The Cape Verde Atmospheric Observatory (CVAO, 16° 51′ 49 N, 24° 52′ 02 W), downwind of the Mauritanian upwelling region with high marine biological productivity, offers the rare opportunity for ground-based studies of clean marine air. Although CVAO is generally considered as representative for the remote marine boundary layer, it is also possible to observe the influence of anthropogenic emissions from long–range transport from North-America and Europe,[38] while the populated islands upwind are not considered as source regions.

4 Results and discussion

For our analysis of the influences of islands on the CH_2Br_2 and $CHBr_3$ distribution, ocean surface measurements are evaluated first followed by an assessment of the ocean interior data. Highest and lowest concentrations are identified and compared to the previously discussed oceanographic and biogeochemical parameters.

4.1 Halocarbon ocean surface distributions

High $CHBr_3$ was measured around the Canaries, where several samples exceeded 100.0 pmol L^{-1} (Fig. 8 and 9 top right).

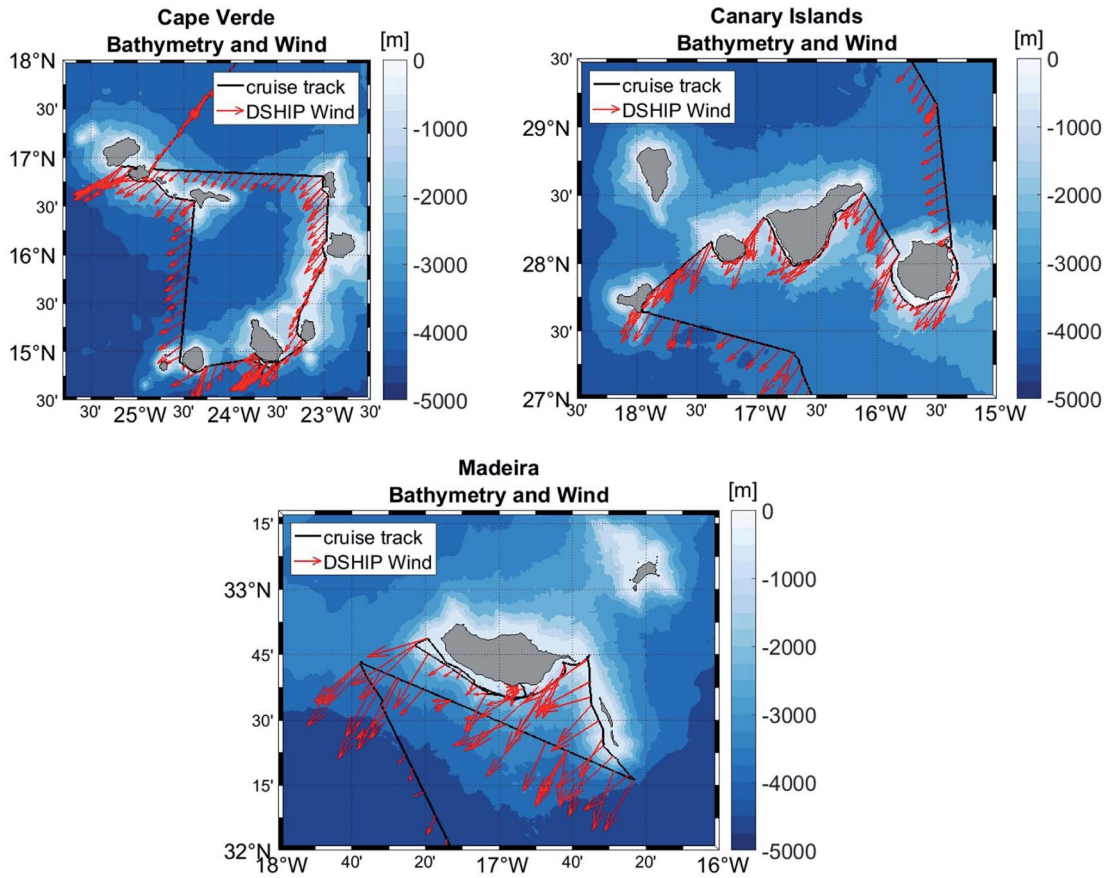

Fig. 7 Normalized wind direction and speed (red arrows) along cruise track (black line) of POS533. The lengths of the legend arrow (DSHIP wind) is 10 m s^{-1} for reference.

Similar high concentrations were found in the harbours of Mindelo with 241.5 pmol L^{-1} and Funchal 314.1 pmol L^{-1}, while the highest concentration during the cruise of 1480.0 pmol L^{-1} was measured in Las Palmas harbour. $CHBr_3$ reached 63.4 pmol L^{-1} at the south of Santiago and was elevated around 30 pmol L^{-1} between 22–24°N during the first transit, between Cape Verde and the Canaries. Low $CHBr_3$ surface concentrations of <10 pmol L^{-1} were found in all areas, except for the Canaries, while Madeira showed the lowest concentrations <5 pmol L^{-1}.

Highest CH_2Br_2 concentrations at Cape Verde often exceeded 10.0 pmol L^{-1}, specifically around the western and southern islands (Fig. 8, top left). It was also high in the harbours with 36.5 pmol L^{-1} in Mindelo, 21.1 pmol L^{-1} in Funchal and 31 pmol L^{-1} in the Las Palmas harbour sample. Similar to $CHBr_3$, CH_2Br_2 was elevated with around 8.0 pmol L^{-1} between 22–24°N during the transit, and low concentrations of <5 pmol L^{-1} were found in all regions, while the lowest concentrations were again detected in Madeira waters.

The ratio of $CHBr_3$ to CH_2Br_2 sea-surface concentrations was highest at the eastern Canary Islands, with frequent ratios above seven, exceeding 15 (Fig. 9, bottom), while the highest ratio of 48 is found in Las Palmas harbour. Few high ratios >10 were also found at Santiago, the largest islands of the Cape Verdes and around 31°N between the Canaries and Madeira during the second transit, as well as in the harbour of Funchal. Ratios between 2 and 4 are typical for open ocean areas, while ratios smaller than 2 were encountered in Madeira waters and ratios around 1 and below were frequent for the Cape Verde surface waters.

The average $CHBr_3$ concentration around Cape Verde was 13.6 pmol L^{-1} excluding harbour samples. The average $CHBr_3$ sea surface concentration around the Canaries was 38.9 pmol L^{-1} and around Madeira, the average for $CHBr_3$ concentrations was 7.9 pmol L^{-1} (Fig. 8 and 9, Table 1).

Cape Verde CH_2Br_2 sea surface concentrations were on average 6.5 pmol L^{-1} (Fig. 9, top left). The mean around the Canaries was 4.8 pmol L^{-1}, while around Madeira the low CH_2Br_2 measurements contribute to a mean of 3.1 pmol L^{-1}.

The mean $CHBr_3$ to CH_2Br_2 ratio around the islands of Cape Verde was 2.4, including the high ratio of 12.9 at the south of Santiago (Fig. 10, top left and right). Around the Canaries, the halocarbon ratio was high with 6.6, as it includes several ratios above 10. Near El Hierro the ratio of $CHBr_3$ to CH_2Br_2 was near 8 and around La Gomera the ratio ranged from 4 to 12. At Tenerife some samples displayed a $CHBr_3$ to CH_2Br_2 ratio of 14, and at Gran Canary all but one sample had a ratio above 15.

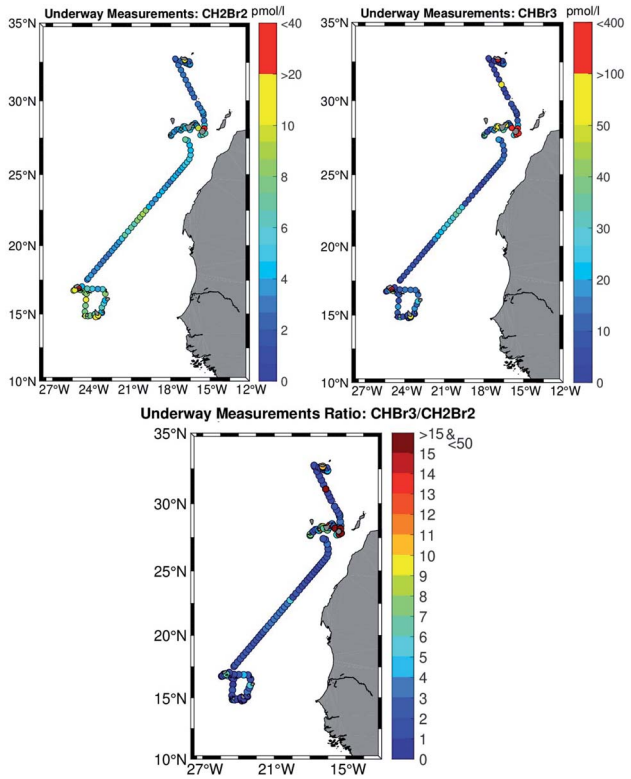

Fig. 8 Top left: CH_2Br_2, top right: $CHBr_3$ underway sea surface data along the POS533 cruise track. Bottom: Underway $CHBr_3$ to CH_2Br_2 ratio along cruise track.

The ratio of $CHBr_3$ to CH_2Br_2 for Madeira was lower than 2 in most locations and showed an average of 2.4, the same as for the Cape Verdes, but with much lower water concentrations of both compounds.

4.2 Halocarbons in the atmosphere

High $CHBr_3$ mixing ratios (>4.0 pptv) were found at all three island groups and during the first transit at approx. 27°N and between 22–24°N (Fig. 11, right). Lowest $CHBr_3$ mixing ratios (<1.5 pptv) were found in open ocean areas at farther distances from coasts. $CHBr_3$ air mixing ratios were more variable than those of CH_2Br_2 (Fig. 11). The highest mixing ratios of $CHBr_3$ in the Cape Verde islands were found south of Sal, southwest of Santiago and north of Sao Nicolau, all in the range of 4.6–5.8 pptv (Fig. 11, top right). At the most western tip of Tenerife, $CHBr_3$ was 7.3 pptv, the highest sample taken throughout the study area. Another high $CHBr_3$ air measurement was found to the west of La Gomera (4.7 pptv). $CHBr_3$ air mixing ratios were also elevated around Gran Canary at approximately 2.7 pptv. Air mixing ratios for $CHBr_3$ around Madeira were lowest with values around 1 pptv and even below. The only exception was at Funchal harbour where atmospheric $CHBr_3$ was high (4.1 pptv, Fig. 11, bottom right).

CH_2Br_2 air data were highest around Cape Verde and at approx. 27°N, generally ranging between 1.5 and 1.7 pptv (Fig. 11, left). Cape Verde atmospheric CH_2Br_2 mixing ratios were highest north of Fogo (1.8 pptv). Other elevated CH_2Br_2 mixing ratios were found between the islands of Maio and Sal and north of Sao Nicolau. All locations around Cape Verde that had elevated atmospheric $CHBr_3$ mixing ratios also showed elevated atmospheric CH_2Br_2. At Santiago, where $CHBr_3$ reached 4.7 pptv the equivalent CH_2Br_2 mixing ratio was 1.7 pptv. Slightly elevated CH_2Br_2 air mixing ratios of around 1.5 pptv were also found between 22 and 24°N. Atmospheric CH_2Br_2 mixing ratios around the Canary Islands were in general lower between 1.1 and 1.4 pptv and were around 0.3 pptv higher in the west than in the east. The highest value was 1.7 pptv in the west of La Gomera. Mixing ratios of CH_2Br_2 around Madeira were consistently below 1.2 pptv.

The atmospheric $CHBr_3$ to CH_2Br_2 ratios (Table 1) were generally between 1 and 2, while the decreased below one in the Madeira region.

4.3 Halocarbon air–sea fluxes

The halocarbon mixing ratios in air were used to calculate the air–sea flux of $CHBr_3$ and CH_2Br_2 during POS533. A positive flux indicates halocarbon transport from the ocean to the atmosphere and is hereafter called sea-air flux.

The strongest $CHBr_3$ fluxes were found at the Canaries, specifically at Tenerife and Gran Canary (Fig. 12, bottom). This caused a weak positive South-North gradient in the $CHBr_3$ fluxes from the southern Cape Verdes towards the northern Archipelagos, with an overall increase of 96.15 pmol m^{-2} h^{-1} along the cruise track. Towards the end of the sampling in Madeira, the $CHBr_3$ flux values increased, similar to the CH_2Br_2 flux (Fig. 12, top) approaching Funchal. On average, the $CHBr_3$ flux values were about 10 times higher than the CH_2Br_2 flux values. Both compounds were emitted from the ocean throughout the cruise, with few values around zero, indicating an equilibrium between ocean and atmosphere. The CH_2Br_2 flux was highest (>5000 pmol m^{-2} h^{-1}) at the beginning of the cruise around the Cape Verde islands. There was a negative South-North Gradient between the southern Cape Verdes and the northern islands with a mean overall decrease along the cruise track (15–32°N) of 80.8 pmol m^{-2} h^{-1}. The sea-air fluxes of CH_2Br_2 and $CHBr_3$ also increased around 22–24°N. $CHBr_3$ fluxes around Cape Verde were generally around 1000 pmol m^{-2} h^{-1}, occasionally above 5000 pmol m^{-2} h^{-1} and some peaks of >10 000 pmol m^{-2} h^{-1} around the islands (Fig. 13, top right). The higher fluxes were found in the south of Sao Vicente, the southeast of Fogo, the south of Santiago and Boa Vista, and northwest of Sal.

High winds during the transit with intermediate water concentrations caused fluxes between 1000 and 8000 pmol m^{-2} h^{-1}. Around the Canaries, the sea-air flux of $CHBr_3$ often ranged between 100 and 1000 pmol m^{-2} h^{-1}, exceeded 10 000 pmol m^{-2} h^{-1} at several places and reached 50 000 pmol m^{-2} h^{-1} between Tenerife and Gran Canary (Fig. 13, middle right). Fluxes for the Madeira stations were on average lower than from locations around Cape Verde and the Canaries (Fig. 13, bottom right). The fluxes in the harbours of Mindelo, Funchal and Las Palmas could range between 10 000 and exceed 100 000 pmol m^{-2} h^{-1}, depending on the wind speed. With a medium wind speed of 7 to 9 m s^{-1} the fluxes would range between 20 000 to 50 000 pmol m^{-2} h^{-1}.

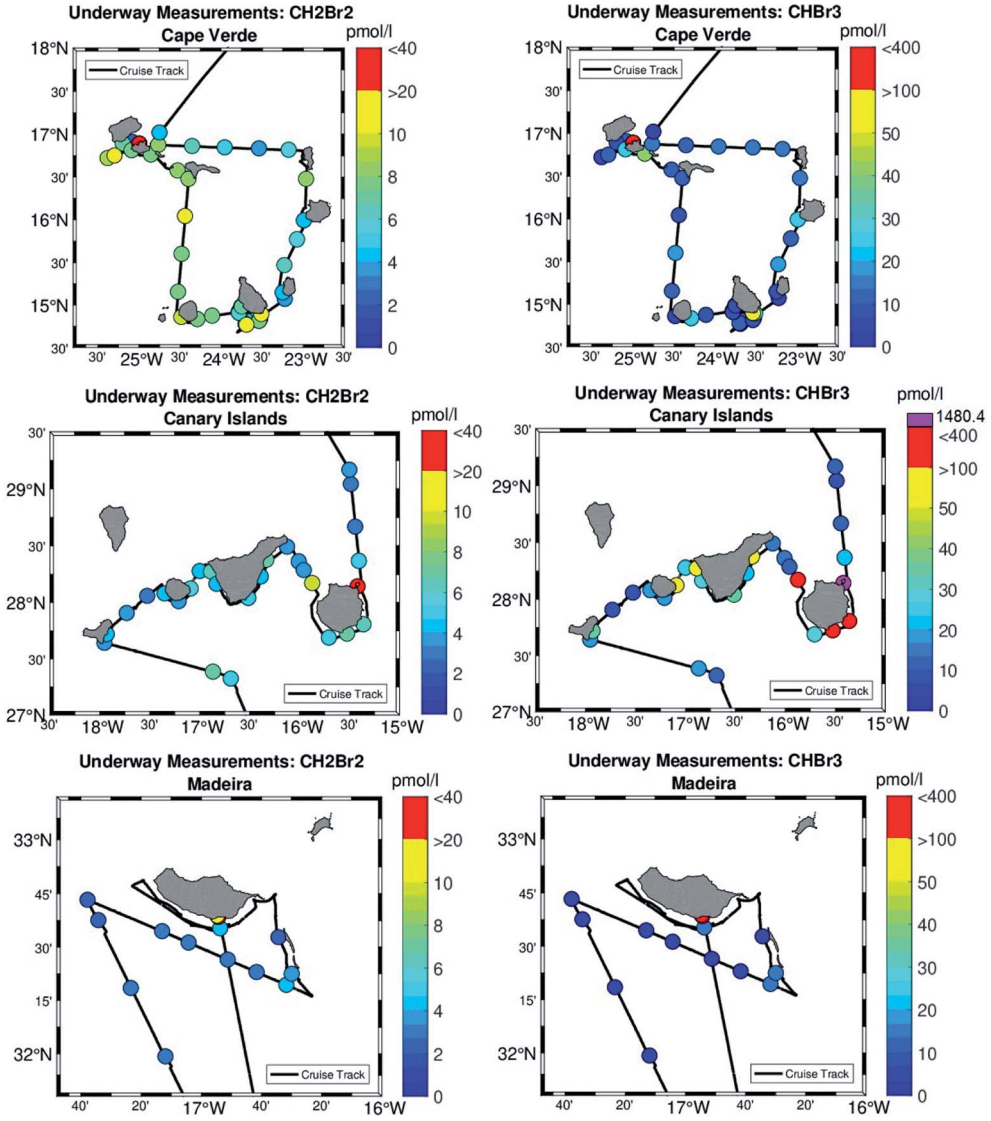

Fig. 9 CH_2Br_2 and $CHBr_3$ underway measurements along POS533 cruise track (black line). Top figures: Cape Verde samples, middle figures: Canary Islands samples, bottom figures: Madeira samples.

CH_2Br_2 sea-air fluxes from Cape Verde were highest in the south of Santo Antao, where the flux was above 4000 pmol m^{-2} h^{-1} (Fig. 13, top left), followed by fluxes from 3000–4000 pmol m^{-2} h^{-1} off the southern coast of Sao Nicolau, southeast of Fogo, and in the south of Santiago. Frequently fluxes >2000 pmol m^{-2} h^{-1} occurred between the islands. During the transit 500 to 2000 pmol m^{-2} h^{-1} were caused by the high wind speeds and varying water concentrations.

At the Canary Islands, CH_2Br_2 sea-air fluxes were generally between 100 and 1000 pmol m^{-2} h^{-1} (Fig. 13, middle left) due to low CH_2 Br_2 concentrations and varied due to the varying wind. Flux values around Madeira for CH_2Br_2 were even lower between 100 and 200 pmol m^{-2} h^{-1}. The CH_2Br_2 fluxes at the harbours could range between 1000 and 12 000 pmol m^{-2} h^{-1} (Fig. 13, bottom left) and would range between 2000 and 6000 pmol m^{-2} h^{-1} at intermediate wind speeds between 7 and 9 ms^{-1}.

4.4 Halocarbon water column distribution

The halocarbon distribution in the upper ocean was analyzed to identify whether highest concentrations were found in the chlorophyll maximum or if other factors were affecting the halocarbon concentrations. Fig. 14 displays both CH_2Br_2 and $CHBr_3$ concentrations in the upper 250 m of the water column. Samples taken below 250 m showed only very low concentrations and were excluded from this analysis.

At Cape Verde, upper ocean $CHBr_3$ concentrations were overall lower in the west than in the east (Fig. 14a). $CHBr_3$ concentrations were highest between 40–80 m depth, where concentrations were above 20 pmol L^{-1} in many sample locations. This corresponds well with the fluorescence and accordingly the chlorophyll maximum at 50–60 m depth (Fig. 19 in Appendix). Three $CHBr_3$ profiles were showing extremely high concentrations (40–220 pmol L^{-1}) at Sal and in

Table 1 Halocarbon water concentrations, atmospheric mixing ratios, and air–sea fluxes during POS533. The harbour samples: Mindelo (28.2.19), 36.5, 241.5, Las Palmas (14.3.19): 31.0, 1480.0 and Funchal (19.3.19): 21.1, 314.1 pmol L^{-1} for CH_2Br_2 and $CHBr_3$ respectively are not included in the table values

		CH_2Br_2_water/ pmol L^{-1}	$CHBr_3$_water/ pmol L^{-1}	Ratio-water	CH_2Br_2_air/ pptv	$CHBr_3$_air/ pptv	Ratio-air	CH_2Br_2_flux/pmol m^{-2} h^{-1}	$CHBr_3$_flux/pmol m^{-2} h^{-1}
Cape Verde	Maximum	14.7	63.4	12.9	1.8	5.8	3.4	5118.4	15 044.8
	Minimum	2.0	3.6	0.6	1.3	1.7	1.2	1.1	−7.7
	Mean	6.5	13.6	2.4	1.5	2.7	1.8	1350.7	2440.6
Transit	Maximum	8.9	34.3	5.4	1.8	4.2	2.3	2373.1	8434.6
	Minimum	2.8	6.0	1.7	1.2	1.3	1.0	313.9	574.3
	Mean	4.7	13.7	2.8	1.4	2.0	1.4	833.3	2432.5
Canaries	Maximum	9.9	285.7	29.0	1.7	7.3	4.6	1623.6	50 927.4
	Minimum	3.0	7.0	2.3	1.1	1.2	1.1	2.6	17.6
	Mean	4.8	38.9	6.6	1.3	2.4	1.7	601.2	6322.2
Madeira	Maximum	4.3	16.5	4.5	1.2	1.6	1.4	886.4	3678.5
	Minimum	2.3	3.8	1.5	1.1	0.9	0.8	26.3	37.1
	Mean	3.1	7.9	2.4	1.2	1.3	1.1	301.3	1091.9
POS533	Maximum	14.7	285.7	29.0	1.8	7.3	4.6	5118.4	50 927.4
	Minimum	2.0	3.6	0.6	1.1	0.9	0.8	1.1	−7.7
	Mean	5.1	18.5	3.5	1.4	2.2	1.6	874.7	3081.4

the north of Boa Vista (yellow and orange circles). Fluorescence data (Fig. 19 in Appendix) confirms that the highest level of biological productivity occurred at this depth and location.

Cape Verde CH_2Br_2 water column measurements displayed an increase in CH_2Br_2 concentrations below the MLD (mean: 40.9 m) beyond the chlorophyll maximum between 50 and 60 m (Fig. 14). Highest CH_2Br_2 concentrations between 10 and 16

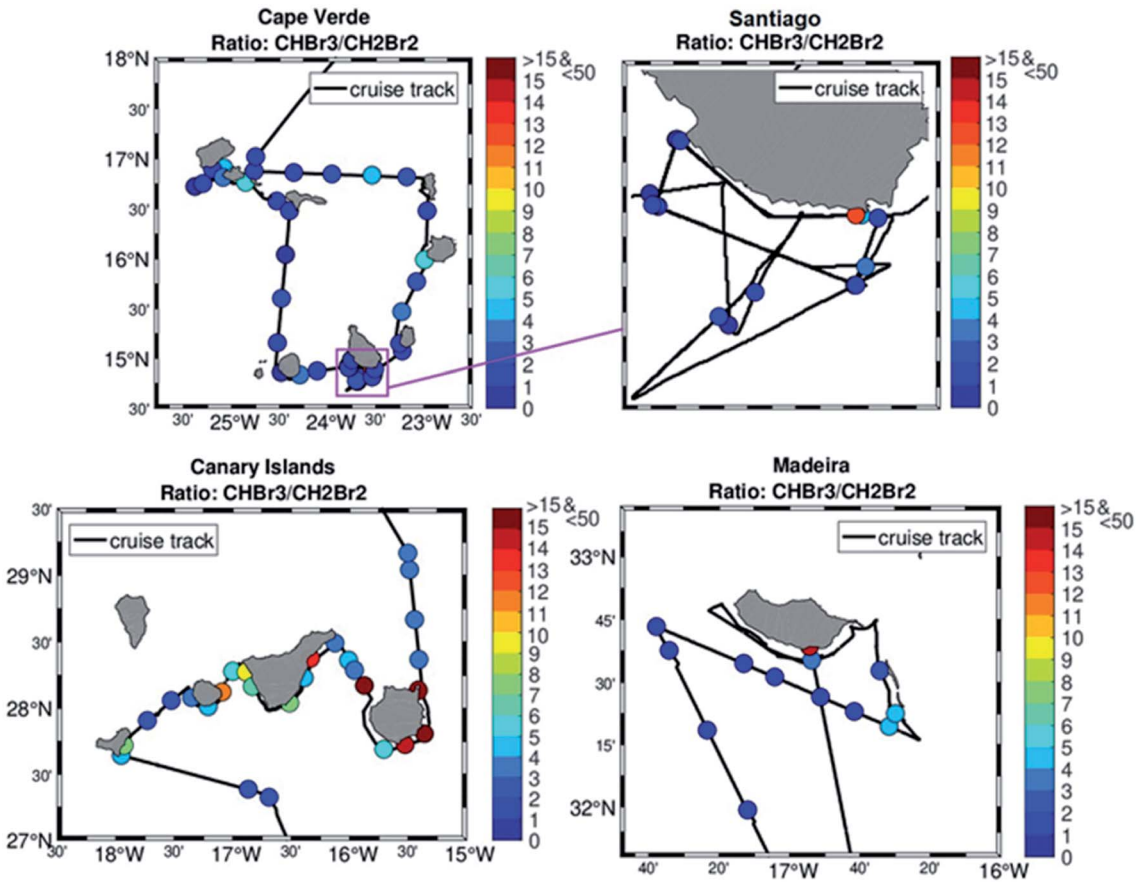

Fig. 10 $CHBr_3$ to CH_2Br_2 ratio along POS533 cruise track (black line). Top figures: Cape Verde samples (left) and Santiago study (right), bottom figures: Canary Island samples (left) and Madeira samples (right).

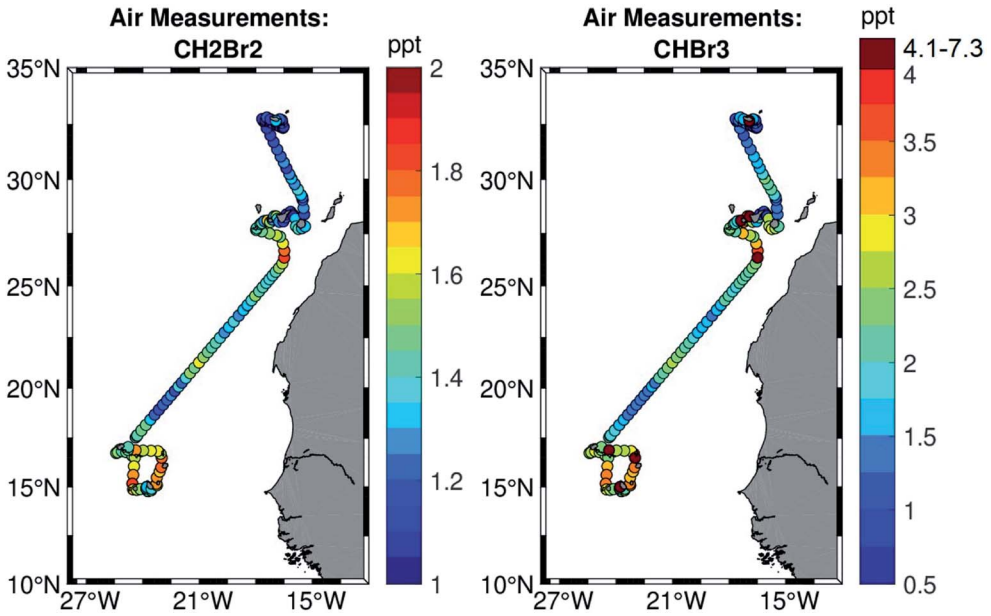

Fig. 11 Halocarbon air measurements along the POS533 cruise track. Right: Dark red circles are included in the foreground to display extremely high data. Left: this procedure was not applied here as CH_2Br_2 measurements do not differ much.

pmol L^{-1} ranged from a depth of 80 to 140 m. One extreme CH_2Br_2 concentration of 26 pmol L^{-1} was found northeast of Sao Vicente (red color-coding).

Water column $CHBr_3$ concentrations at the Canaries ranged from 5 pmol L^{-1} to over 110 pmol L^{-1} (Fig. 14b). A weak increase of $CHBr_3$ water concentrations towards the east was

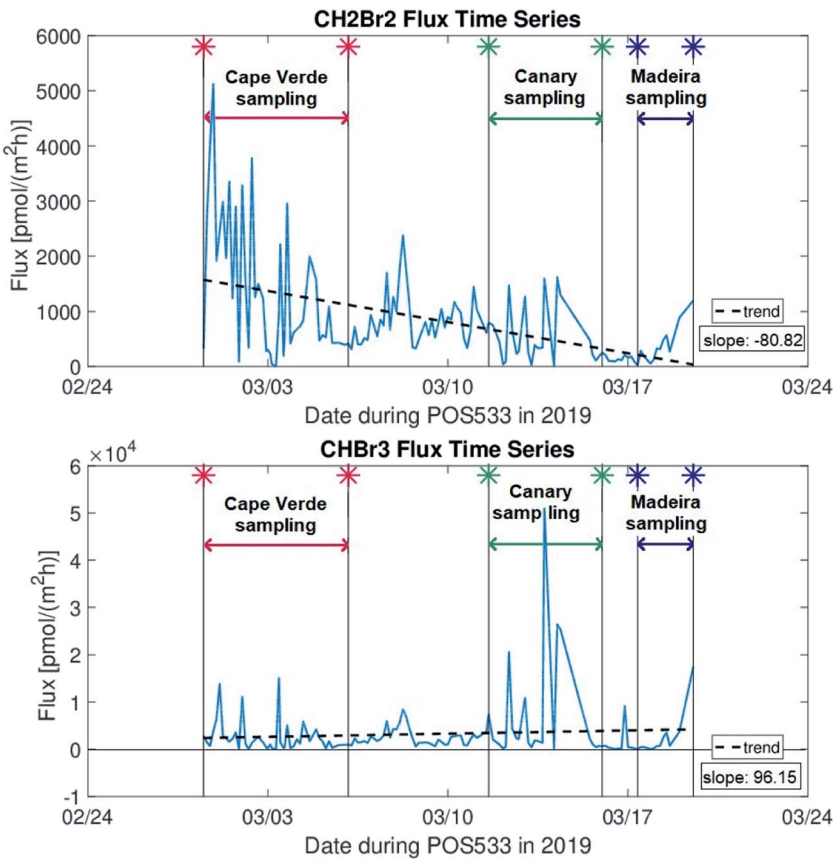

Fig. 12 Ocean-Atmosphere flux against time during POS533 cruise. Colored stars indicating time period of Cape Verde (red), Canary Island (green) and Madeira sampling (blue).

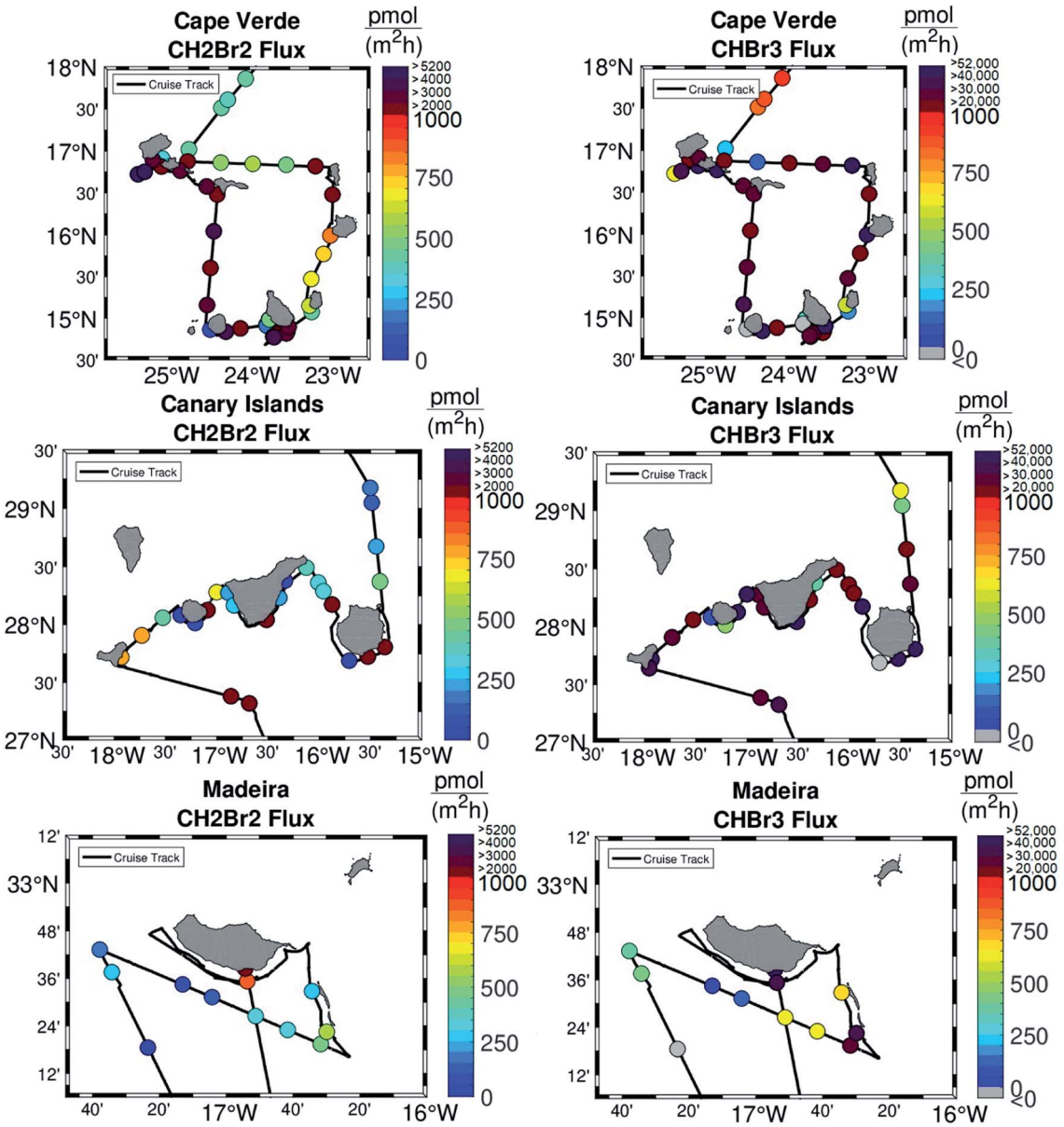

Fig. 13 CH_2Br_2 and $CHBr_3$ flux measurements along POS533 cruise track (black line). Top figures: Cape Verde samples, middle figures: Canary Island samples, bottom figures: Madeira samples.

identified and the eastern stations at El Hierro and La Gomera (blue circles) showed lowest concentrations, followed by most of the Tenerife profiles (green to yellow circles) and highest concentrations were located around Gran Canary (orange and red circles). Elevated $CHBr_3$ concentrations at around 50 m and increased fluorescence data at this depth are coherent. However, upper ocean fluorescence at the Canaries was much weaker than it was at Cape Verde. Elevated $CHBr_3$ concentrations (>80 pmol L^{-1}) at around 50 m were found to the south of Tenerife (light green circles). Only two stations displayed higher concentrations, both located at Gran Canary (80–120 pmol L^{-1}). Whereas surface fluorescence at the Canaries was low, the high $CHBr_3$ concentrations at 30–70 m depth were consistent with elevated fluorescence data at this location (Fig. 19). It appears at the Cape Verde and the Canary islands, that many stations show maximum concentrations between 15 and 20 pmol L^{-1} in all depth ranges, whereas some stations stand out with higher concentrations.

Upper ocean halocarbon distribution around the Canaries displayed a smaller range of CH_2Br_2 concentrations from 2 to 10 pmol L^{-1} and no increasing CH_2Br_2 concentrations beneath the chlorophyll max, as found around Cape Verde. Only one station in the south of Tenerife showed this trend, where the maximum concentration (~9 pmol L^{-1}) was at around 50 m depth, similar to the corresponding $CHBr_3$ profile. A comparison with the fluorescence data at this location showed a local increase in biological productivity.

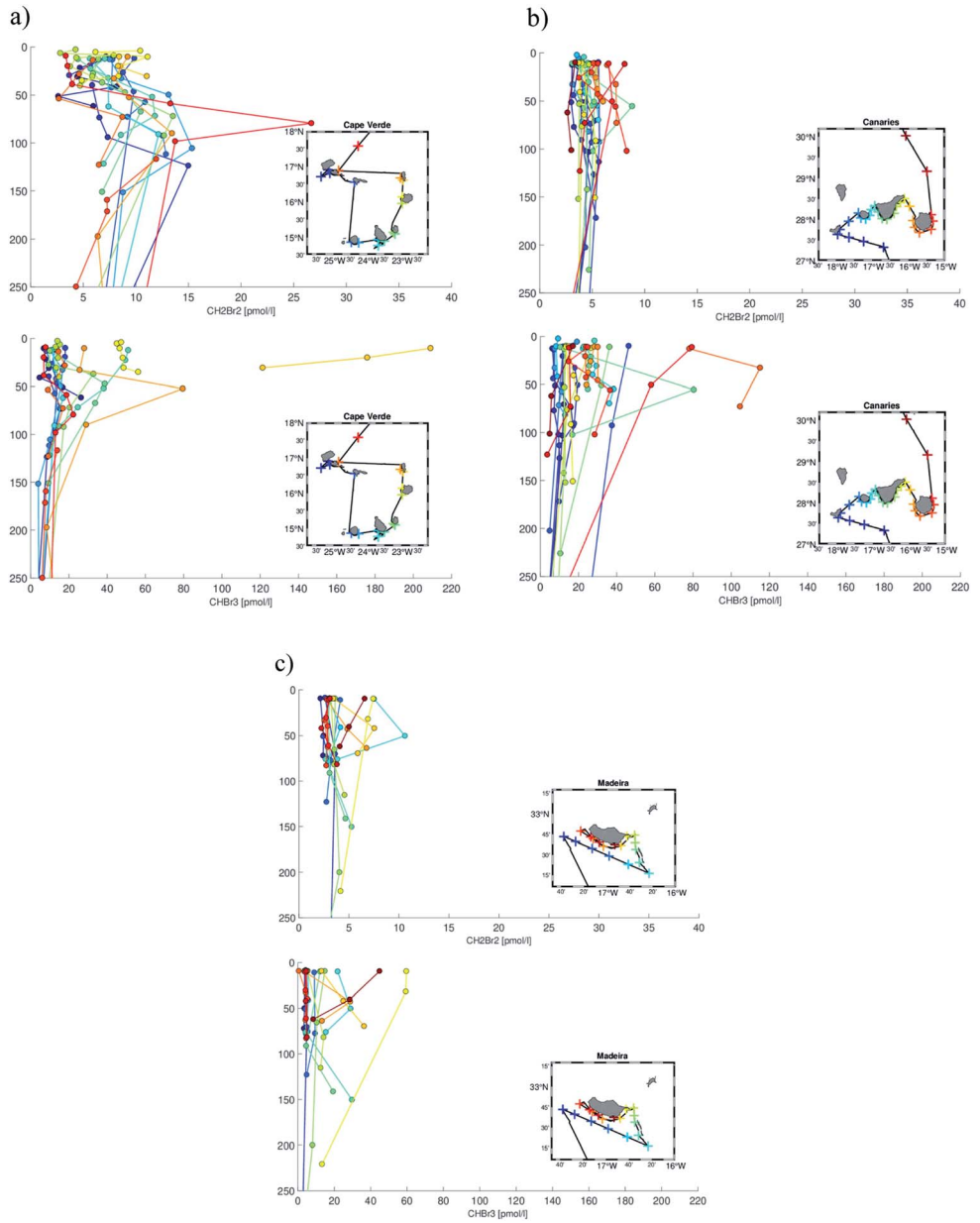

Fig. 14 Concentrations of bromocarbons in the upper 250 m (axis in m) of the water column at (a) Cape Verde, (b) the Canaries and (c) Madeira. CH_2Br_2 (top panel) and $CHBr_3$ (bottom panel). The circles indicate the sampling locations in the water column. The colored lines are used only for better visualization of the relative halocarbon concentrations between locations. The color coding corresponds to CTD locations shown in inset map.

$CHBr_3$ concentrations at Madeira displayed two concentration maxima (Fig. 14c). One was located at around 40–80 m depth (20–40 pmol L^{-1}) which was still in the mixed layer (MLD Madeira: 94.3 m), and a second at around 130–150 m depth (20–35 pmol L^{-1}). The highest $CHBr_3$ concentrations were found in the upper 30 m at the most eastern tip of the island reaching up to around 60 pmol L^{-1}.

CH_2Br_2 measurements around Madeira were generally below 5 pmol L^{-1} and had the lowest average in comparison to the other island groups. A slight increase in the concentrations was found at the most eastern tip of the island at depth ranging from 10–70 m and concentrations between 5 and 1 2 pmol L^{-1}. The maximum CH_2Br_2 concentration was also located at the most eastern tip of the cruise track (turquoise circles), reaching nearly 12 pmol L^{-1}.

4.5 Discussion on halocarbon emissions and sources in the Macaronesian region

Ratios between the atmospheric mixing ratios of two or more halocarbons have been used in the literature to estimate regional and global oceanic halocarbon fluxes.[40,67,68] The studies report linear relationships and correlations between the mixing ratios of $CHBr_3$ and CH_2Br_2 of 0.74 and 0.76.[40,67] This indicates

that these substances share the same sources, and a correlation of 0.91 can be reached in the open ocean atmosphere.[68] All three studies arrived at "global" emission ratios from seawater for $CHBr_3$ to CH_2Br_2 of 9, and deduce common oceanic sources for the compounds. $CHBr_3$ concentration-dependent changes in the atmospheric concentration ratios have been discussed mostly in terms of differences in the chemical reactivities of CH_2Br_2 and $CHBr_3$ in the atmosphere. Changes in the concentration of $CHBr_3$, which has a relatively short atmospheric lifetime of around two weeks, are expected to be more pronounced than changes in the concentrations of the longer-lived CH_2Br_2, with an atmospheric lifetime of around three months. A decrease in the ratio is thus consistent with more aged air masses, in which $CHBr_3$ has been preferentially removed.[40] Alternatively, the change in ratio is also consistent with dilution of the original air mass into a background with higher CH_2Br_2 (a likely situation since CH_2Br_2 is longer lived). These studies only consider ratios in the atmosphere and infer emissions from the oceans, but make no assumptions or conclusions about the initial sources. Brinckmann *et al.*[68] concede that during the initial emission from the algae species into the ocean water deviating abundance ratios are expected,

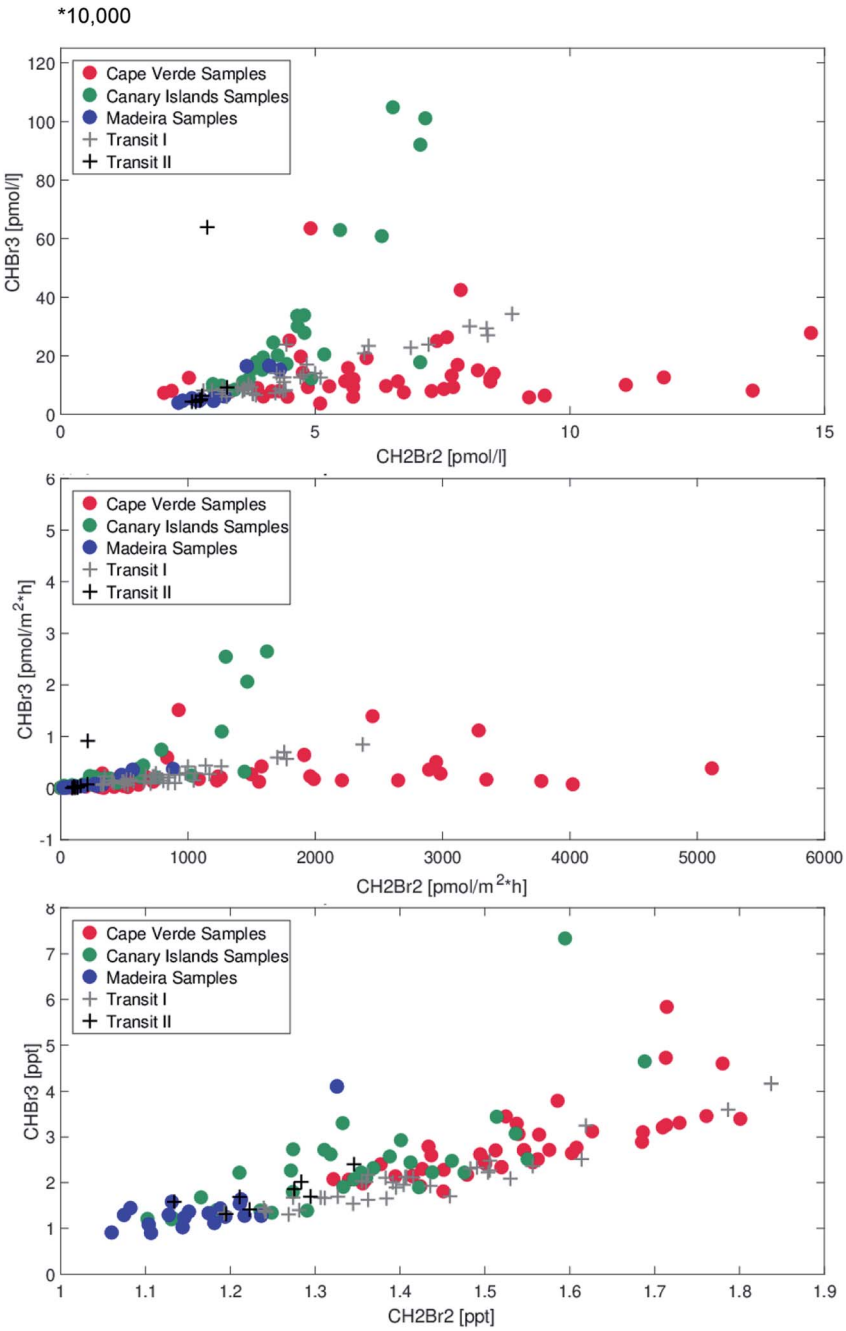

Fig. 15 *X*/*Y*-Plots of bromoform ($CHBr_3$) *versus* dibromomethane (CH_2Br_2) for oceanic surface concentrations during POS533, air–sea fluxes and atmospheric mixing ratios. Locations of samples are color-coded.

Table 2 Pearson rank coefficients (R^2) of fluorescence (arbitrary units), CH_2Br_2 and $CHBr_3$ for individual data pairs in the different regions, the entire cruise and for the means of each region

	Fluorescence (mean)	Fluorescence/ CH_2Br_2	Fluorescence/$CHBr_3$	$CHBr_3$/CH_2Br_2
Cape Verde	254.7	0.0278	0.0019	0.0117
Transit 1	160.8	0.1332	0.2278	0.8643
Canaries	145.6	0.0001	0.0157	0.7319
Transit 2	147.1	0.7537	0.0903	0.0496
Madeira	154.6	0.5425	0.5751	0.8184
POS533 (all data)	188.7	0.1505	0.0108	0.0893
Regional means	175.3	0.6552	0.0563	0.0673

due to different rates of degradation in the surface water prior to the emission through the sea surface. The authors state, considering that it is not possible to collect any emission gas before it has become mixed and diluted, the emission ratio might even be higher.

Knowledge about the oceanic sources however is crucial to infer their future development. In the following we discuss the halocarbon distribution, the emission ratios and their sources and the implications. During the cruise of POS533 the mean ratio of $CHBr_3$ to CH_2Br_2 in the atmosphere was 1.6, with a range from 0.8 to 4.6. The ratio between the seawater concentrations showed a mean of 3.5, and a much larger range of 0.6 to 29. The ratio between the $CHBr_3$ to CH_2Br_2 sea-air fluxes, with a similar mean of 3.9 span a range of 0.1 to 43, while ratios above 6 are rare (Fig. 15).

For interpretation of halocarbon sources during POS533, the ratio between $CHBr_3$ and CH_2Br_2 seawater concentrations will be used (Fig. 10) in combination with the concentration distributions. To make assumptions about the sources, a comparison of halocarbon concentrations and ratios to chlorophyll α and fluorescence was used to identify natural production regions. Data from the POS533 cruise suggest that some areas appear as natural production regions of CH_2Br_2 and $CHBr_3$. This is evident as the data show a good conformity between elevated halocarbon concentrations (individual data and regional means, Table 2) and fluorescence (proxy for chlorophyll α and phytoplankton abundance) in these regions. Hepach *et al.*[21] calculated the correlation coefficient R^2 at the 95% confidence level between CH_2Br_2 and $CHBr_3$ with chlorophyll α to be 0.49 and 0.38 at Cape Verde and the Canaries. During POS533 the R^2 of fluorescence and CH_2Br_2 was high during the second transit and in Madeira waters and it was also high between the regional mean values for CH_2Br_2 and fluorescence (Table 2). The

Table 3 Prior data from publications on $CHBr_3$ and CH_2Br_2 in atmosphere and ocean of the study region

Study	Region	Time	$CHBr_3$ (pmol L^{-1})	CH_2Br_2 (pmol L^{-1})	$CHBr_3$ (pptv)	CH_2Br_2 (pptv)
Class *et al.*[43]	24°N 18°W	March 1985	>24	>5	0.8–2.6	1.0–2.4
Class *et al.*[44]	Tenerife Beach	October 1985	4	2	43 988	2.6–3.6
Class *et al.*[44]	Azores beach	June 1982			460	50
Class and Ballschmiter[45]	30–40°N	March 1985			2	2
Fischer *et al.*[47]	West of Canary islands	June 1998			<1	
Ekdahl *et al.*[48]	Isolated rockpool (10 m^3) at Tenerife, Taliarte with macroalgae	August 1993	500–5000	100–700	2000–26 000	37–340
Quack *et al.*[20,27]	Mauritanian upwelling (16–19°W, 17–21°N)	March 2005	5.2–23.8	3.1–7.0	3.1–11.8	1.7–3.4
Carpenter *et al.*[41]	Mauritanian upwelling (17–21°W, 8–25°N)	October/November 2002			4–13	
Carpenter *et al.*[39]	Canaries (between Tenrife and Gran Canary)	May–June 2007	14.4	3	0.7	0.2
O'Brien *et al.*[40]	Cape Vere Atmospheric Observatory (coastal)	May–June 2007			2.0–43	1.7–3.2
Lee *et al.*[38]	Cape Vere Atmospheric Observatory (coastal)	26. May 2007			0.1–4	0.3–0.6
Fuhlbrügge *et al.*[42]	Mauritanian upwelling (16–24°W, 17–20°N)	June 2010			1–8.9	0.7–3.1
Liu *et al.*[74]	Canary region (16–20°W, 27–31°N)	October/November 2010	1–30	1.5–6	0.5–3.5	0.7–1.5
Hepach *et al.*[21]	Mauritanian upwelling (16–24°W, 17–20°N)	June 2010	1–42.4	1–9.4	1–8.9	0.7–3.1

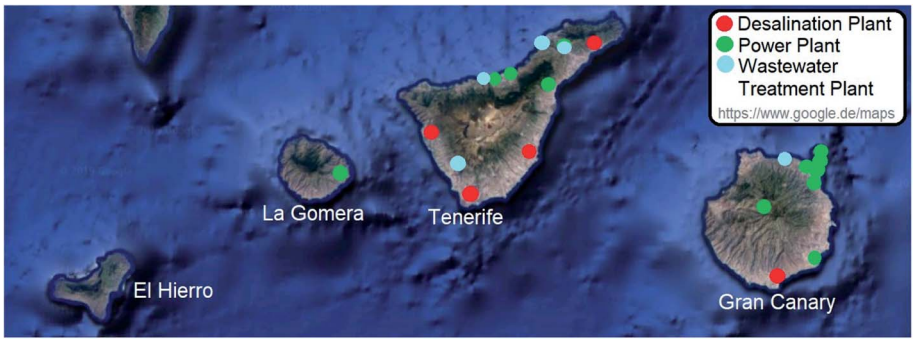

Fig. 16 Locations of desalination, power and wastewater treatment plants at the Canary Islands (Google Earth 2019).

correlation coefficients for CHBr3 with fluorescence where much weaker, except for Madeira waters. The correlations between the compounds concentrations varied strongly between the regions (Table 2).

At Cape Verde and during the first transit, the $CHBr_3$ to CH_2Br_2 concentration ratio in seawater was generally smaller than 3 and concentrations of the compounds were moderate, between 4 and 14 pmol L^{-1} for CH_2Br_2 and 7 and 27 pmol L^{-1} for $CHBr_3$. Concentrations of $CHBr_3$ in all regions and most samples where below 30 pmol L^{-1}. Where the concentrations were elevated, they were larger than 60 pmol L^{-1}. When the concentrations increased, the ratio between $CHBr_3$ and CH_2Br_2 also increases from values below 7 to values above 9. In the harbours the concentration ratios ranged from 8 to 48. As harbours most likely contain anthropogenic sources of halocarbons,[11,34] we estimate a ratio of larger than 8 as an indicator for anthropogenic influence with predominant $CHBr_3$ sources.

For macroalgae, the average emission ratios between $CHBr_3$ and CH_2Br_2 of 13.5 (±7.9) for $CHBr_3$ to CH_2Br_2 was calculated from emission rates summarized by Carpenter and Liss.[23] As a ratio in coastal seawater, influenced by seaweed, the authors report a ratio of $CHBr_3$ to CH_2Br_2 of 7.8. This is consistent with our observed ratios, and macroalgae have been named as sources for the compounds in the region,[44,45,48] thus we discuss the likelihood of macroalgae as sources for the high concentrations and ratios in the region.

The Macaronesian region, in general, is a Biodiversity Hotspot included in the Mediterranean Basin.[69] The biodiversity of macroalgae around the Archipelagos comprises about 950 species.[70] The highest macroalgae diversity is reported for the Canary islands with 689 species,[71] followed by the biogeographically close related Selvagens and Madeira archipelagos (295 and 396 spp., respectively). Despite of similar species numbers, the Azores and Cape Verde islands are biogeographically quite distinct, representing the northernmost and southernmost boundaries with cold-temperate and tropical affinities, respectively, in terms of community composition.[72] In terms of overall productivity, the region is falling within the eastern limit of the Northeast Atlantic subtropical gyre with mesotrophic (Azores, Cape Verde) to oligotrophic conditions (Madeira, Canary Islands) with rather low primary production. and low biomass of macroalgae. The abundance of crustose coralline algae (generally low in biomass) which is the most abundant functional type of macroalgae, is decreasing from Cape Verde towards Madeira, mainly due to various degrees of herbivory.[72] The perennial macroalgae of all Macaronesian Archipelagos are on decline, as they are threatened by tourist activities and islands water discharges.[73] Macroalgae environments generally emit only nanomolar concentrations to the surrounding waters, even when the standing stock of biomass is larger than in the subtropical Macaronesian region.[23,24] While we cannot completely rule out the contribution of macroalgae as a source for the compounds, we assume their contribution marginal compared to the anthropogenic contribution in the waters between 50 and 100 m depth around the islands. The contribution of macroalgae to the levels of $CHBr_3$ and CH_2Br_2 needs to be investigated in a follow up study. The elevation of $CHBr_3$ concentrations above 60 pmol L^{-1} is more likely caused by industrial disinfection activities. They all produce $CHBr_3$ as the main product in micro molar concentrations, as in hundred thousands of m^3 cooling waters from coastal power plants,[32] desalination plants,[33] entering the marine coastal waters and in treated ballast water[11] and industrialized urban environments.[34]

4.5.1 Natural causes for elevated halocarbon concentrations. Chlorophyll α was highest around Cape Verde, showed increased values around 22–24°N and slightly increased at Madeira (Fig. 19 Appendix). Both chlorophyll α and fluorescence are potential proxies for oceanic productivity, which is linked to the production of halocarbons.[74,75] The highest surface concentrations of CH_2Br_2 and the lowest $CHBr_3$ to CH_2Br_2 ratios, often between 0 and 2, were found near Cape Verde (Table 1). The concentrations from March 2019 of POS533 (17.0°N) were similar to those measured in June 2010 northeast of Sao Vicente (17.6°N) (Table 3).[21] The Cape Verde region showed also the lowest $CHBr_3$ to CH_2Br_2 ratios in the water column and the highest flux of CH_2Br_2 into the atmosphere. In the following we discuss possible causes for this.

During biological processes in the ocean, $CHBr_3$ is preferentially produced over CH_2Br_2.[39,51] Also the bromination of extracellular dissolved organic matter, has been shown to produce generally $CHBr_3$.[25,26] Towards the open ocean, away from source regions, the ratio between $CHBr_3$ and CH_2Br_2 declines in the surface ocean, due to a faster photolysis of $CHBr_3$ compared to CH_2Br_2 in ocean and atmosphere.[21,23] As

$CHBr_3$ has an increasing sea-air concentration gradient, compared to CH_2Br_2 towards the open ocean, this may lead additionally to a faster loss from the surface waters.[20,27] The POS533 measurements around Cape Verde also showed increasing concentrations of CH_2Br_2 with water column depth, down to 150 m in the thermocline (Fig. 18, top left). The fluorescence maximum for Cape Verde sample stations was at around 50–60 m depth, and therefore covered only part of these elevated concentrations, while the CH_2Br_2 production zone was deeper. In earlier cruises an increase of CH_2Br_2 concentrations and a decline of $CHBr_3$ with depth was observed in the Mauritanian upwelling region as well,[20] $CHBr_3$ was hypothesized to be converted to CH_2Br_2 *via* reductive hydrogenolysis[28] under the less oxic conditions or *via* microbial reduction in the thermocline waters.

Laboratory studies since that time, indicated that the production of CH_2Br_2 from heterotrophic cycling of $CHBr_3$ can be a wide-spread phenomenon in the marine environment.[29–31] The subsequent entrainment of the enriched thermocline waters into the mixed layer can contribute to the ratio shift between $CHBr_3$ and CH_2Br_2 in the open ocean and upwelled waters. In addition the above processes, a lower $CHBr_3$ to CH_2Br_2 production ratio in the open ocean can be another explanation for the decreasing $CHBr_3$ to CH_2Br_2 ratios. A major difference between the Cape Verdes and the other archipelagos, where the increase of CH_2Br_2 with depth was not observed, were the low oxygen concentrations in the thermocline waters (Fig. 8). We therefore hypothesize again, that the high CH_2Br_2 concentrations and fluxes in the Cape Verde region during POS533 are a consequence of microbial reduction of $CHBr_3$ in the low oxygen thermocline waters and that reductive hydrogenolysis is involved. Although this process generally occurs in anoxic conditions, it may also occur in the oxygenated water column, as anoxic processes in oxygen rich waters have been described earlier *e.g.* for methane production in the sea.[76]

The higher CH_2Br_2 atmospheric mixing ratios in the Cape Verde region underline the significance of the marine processes in the water column for the troposphere (Fig. 15).

An increase in chlorophyll α along the first transit from the Cape Verdes to the Canaries affected both CH_2Br_2 and $CHBr_3$ water concentrations and as such increased their sea-air fluxes to the atmosphere. During the first transit at 22–24°N, the $CHBr_3$ to CH_2Br_2 ratio was slightly higher than in the Cape Verde region, reaching up to 6. Here, colder surface temperatures indicate nutrient input, leading to elevated chlorophyll α, which has been observed to coincide with higher $CHBr_3$ and CH_2Br_2 concentrations and an elevated ratio of around 4 in this and other biologically active regions.[21,27,39,74,75,77,78] In comparison to the region around the Cape Verde Archipelago, the fresher upwelling and more oxic conditions possibly lead to this higher $CHBr_3$ to CH_2Br_2 ratio.

Around Madeira, both halocarbons showed low average concentration and calculated ratios were also low in most sample locations. Chlorophyll α was slightly elevated. Halocarbon water concentrations at Funchal harbour were high, thus a strong flux of especially $CHBr_3$ into the atmosphere occurred, which was visible in a high atmospheric mixing ratio of 4 pptv of $CHBr_3$. The low winds in the islands wake support this accumulation.

Around the Canaries no overlaps between elevated halocarbon concentrations and fluorescence or chlorophyll α were observed. The ratios between $CHBr_3$ and CH_2Br_2 were often extraordinary high in these islands, why this island group is therefore further discussed as an area of anthropogenic halocarbon sources.

4.5.2 Anthropogenic influences on halocarbon surface concentrations. The halocarbon surface concentrations at the Canaries were frequently elevated (>60 pmol L^{-1} for $CHBr_3$ and >7 pmol L^{-1} for CH_2Br_2 in 7 locations) relative to other studies from the area.[21,27,39] The mean CH_2Br_2 concentration of Carpenter *et al.*[39] in May–June 2007 around the Canaries was 3.0 pmol L^{-1}, which is similar to the POS533 mean of 4.8 pmol L^{-1}. Their $CHBr_3$ average of 14.4 pmol L^{-1} in open ocean waters between Tenerife and Gran Canary is similar to the POS533 data of 14–18 pmol L^{-1} in the same region. But during POS533 higher values (>100.0 pmol L^{-1}) were measured in close proximity to the coasts of Tenerife and Gran Canary, which were not sampled during prior cruises. $CHBr_3$ concentrations at Las Palmas harbour exceeded 1400 pmol L^{-1}. This pattern of higher concentrations around the coasts and lower concentrations in more open ocean regions was also reflected in the ratio of $CHBr_3$ to CH_2Br_2 (Fig. 9). The ratio was above 9 in many locations around the islands. Despite the strong winds halocarbon mixing ratios in air near the Canaries were also higher than during previous ship based studies. Carpenter *et al.*[39] measured atmospheric $CHBr_3$ of 0.7 pptv and CH_2Br_2 of 0.2 pptv around the Canaries. Average air mixing ratios measured during the POS533 cruise were 2.4 pptv ($CHBr_3$) and 1.3 pptv (CH_2Br_2) in the region and more similar to the values of Liu *et al.*[74] from October 2010. Sea-air fluxes as high as the ones detected during the POS533 cruise around the Canaries from >20 000 and up to 50 000 pmol m^{-2} h^{-1} (Fig. 13 and 15) have not previously been reported for the area and could contribute to the elevated mixing ratios. The largest sea–air flux of Carpenter *et al.*[39] was around 3000 pmol m^{-2} h^{-1} for the Canary region, while their average was around 1700 pmol m^{-2} h^{-1}. Hepach *et al.*[21] calculated 2000 pmol m^{-2} h^{-1} in the coastal upwelling area near Mauritania, The global maximum flux of $CHBr_3$ in Ziska *et al.*[13] is below 200 000 pmol m^{-2} h^{-1}, while their global average is below 250 pmol m^{-2} h^{-1} for $CHBr_3$. Fluxes of >1500 pmol m^{-2} h^{-1} were very high in their climatology, but less than quarter of the mean flux around the Canaries of 6300 pmol m^{-2} h^{-1} (Table 1) during POS533.

At the Canaries, island wake effects caused frequent changes of wind patterns and strengths (Fig. 6 and 7) which was reflected in the fluxes of both $CHBr_3$ and CH_2Br_2. On the windward sites of the Canary islands these fluxes were up to ten times higher compared to the leeward sites, due to the high halocarbon surface concentrations and the elevated wind speeds around the harbours and big cities of the islands. Much higher $CHBr_3$ water concentrations relative to CH_2Br_2 indicate anthropogenic input of halocarbons, as especially anthropogenic sources from disinfection processes contribute preferentially to the load of $CHBr_3$.

Liu *et al.*[74] also measured elevated halocarbon concentrations around the Canaries and suggested that the unique ecosystems of island environments might affect halocarbon production. Chlorophyll α measurements were lowest in this area. Macroalgae, which are also stronger producers of $CHBr_3$ than of CH_2Br_2 (ref. 23) have been suggested as $CHBr_3$ sources in the region of the Canary islands.[43–45,48] Possible anthropogenic input in urbanized coastal oceans may obscure natural variations, as identified around the Gulf of Mexico.[79] Given that halocarbon concentrations were always highest in harbour samples, it cannot be denied that there is anthropogenic input around the islands. As seaweeds produce nanomolar concentrations of $CHBr_3$ in their environment, they cannot be completely ruled out as a contributor of increased $CHBr_3$ concentrations. However as their standing biomass is low (see chapter 4.5) they are unlikely to cause such high concentrations as were found in the surface water around the islands in a distance of around 1 km with 50 to 100 m water depths. Anthropogenic discharges, which are several hundred thousands of m^3 per day and where $CHBr_3$ is found in micromolar concentrations, as in cooling waters from coastal power plants[32] and desalination plants[33] are much more likely as cause.

The anthropogenic influences at the Canaries might be linked to a rise in the tourism-based industry. There has been a continuous rise in tourism over the last decades, with 0.7 million tourists visiting Cape Verde in 2018,[80] 13.1 million tourists in the Canaries in 2016,[81] and 1.3 million tourists in Madeira in 2017.[82] With tourism comes a rise in industry, including an increased number of power plants, wastewater treatment plants, and desalination plants,[83–85] which all release $CHBr_3$.[32–34,37]

Fig. 16 gives an overview of industrial development in the Canaries. Many of these locations correlated with high $CHBr_3$ to CH_2Br_2 ratios and extreme $CHBr_3$ surface concentrations during POS533. For example, the highest ratio and $CHBr_3$ concentration of 62.8 pmol L^{-1} at La Gomera correspond to the location of a power plant. The locations of several desalination plants at Tenerife corresponded with high $CHBr_3$ to CH_2Br_2 ratios and similarly high $CHBr_3$ concentrations were found in the northeast and west of Tenerife (Fig. 12).

At Gran Canary high $CHBr_3$ to CH_2Br_2 ratios were found close to power plants in the north and southeast of the island. These locations also had $CHBr_3$ concentrations in the range of 100 to 1480 pmol L^{-1}, the latter at Las Palmas harbour. The mean sea-air flux for $CHBr_3$ at the Canaries of 6700 pmol m^{-2} h^{-1} was around three times higher as the $CHBr_3$ flux averages measured at Cape Verde and Madeira (2440 pmol m^{-2} h^{-1} and 2530 pmol m^{-2} h^{-1} respectively). These findings in combination with the close proximity to industrial plants support the hypothesis that anthropogenic influences explain the highest halocarbon concentrations at the Canaries.

5 Conclusions

This analysis of island influences on biogeochemical cycles of halocarbons has generated new findings in halocarbon research. The oceanic halocarbon concentrations measured in coastal regions of Cape Verde, the Canaries and Madeira were much higher than found during previous studies in the region.[21,39] These high concentrations were linked to both natural and anthropogenic causes. Cape Verde was found to be an area of rich biological productivity that produces halocarbons in the surface and upper ocean. Upwelling favored biological production conditions, low oxic conditions and microorganisms in deeper waters of the thermocline likely convert $CHBr_3$ to CH_2Br_2. This conversion results in elevated CH_2Br_2 surface water concentrations and small ratios of $CHBr_3$ to CH_2Br_2 around Cape Verde. This region was therefore a significant source of CH_2Br_2 to the atmosphere, which was reflected in the high atmospheric CH_2Br_2 mixing ratios. Around the Canaries an anthropogenic influence on $CHBr_3$ was visible in unique high ratios of $CHBr_3$ to CH_2Br_2, which was likely caused from coastal anthropogenic disinfection processes used in power plants and desalination technologies. $CHBr_3$ concentrations of more than 1400 pmol L^{-1} (Las Palmas harbour), several samples more than 100 pmol L^{-1} (Gran Canary coasts), and a $CHBr_3$ sea-air flux of on average 6700 pmol m^{-2} h^{-1} indicated that industrial discharges likely influence coastal waters and the atmosphere. Elevated halocarbon surface concentrations at Mindelo and Funchal harbours also displayed a visible anthropogenic signal leading to increased flux of the compound from the ocean to the atmosphere.

$CHBr_3$ seawater concentrations of more than 30 000 pmol L^{-1}, much higher than those measured during POS533, and sampled directly near beaches of Tenerife and Gran Canary in May 2019 (unpublished work), confirm the hypothesis that local anthropogenic sources (*e.g.* disinfection processes) elevate near shore concentrations. As $CHBr_3$ is generally the major compound in disinfected seawater, $CHBr_3$ could be used as a tracer for other toxic disinfection byproducts.[86] Macroalgae as sources for the halocarbons in the near-shore waters are less likely, due to their smaller production rates and low abundance in the region.

Wind speed enhances mixing processes and therefore decrease halocarbon surface concentrations in distance to the coast. Furthermore, wind speed positively influences the halocarbon sea-air flux to the atmosphere, which led to on average 4.5–6.6 fold higher halocarbon fluxes on the windward sites of the islands, where wind speeds were on average twice to three times higher as they were leeward of the island. In the windward sites of islands around the Canaries, the sea-air flux was largest, because strongly elevated surface concentrations, containing an anthropogenic signal, contribute to the flux in addition to the strong wind on these sites.

CH_2Br_2 and $CHBr_3$ are important bromine sources to both the troposphere and the lower stratosphere, where they influence tropospheric chemistry and stratospheric ozone depletion. The significance of locally increased fluxes of CH_2Br_2 as detected between the Cape Verdes and of $CHBr_3$ around the Canaries have not been previously described. The atmospheric abundance of the organic bromine compounds $CHBr_3$ and CH_2Br_2 is generally related to common marine sources, which are still insufficiently identified. The cruise revealed that the major sources of both compounds for the atmosphere were spatially

separated between the Macaronesian Archipelagos. $CHBr_3$ sea-air fluxes were dominated by anthropogenic sources, while heterotrophic processes in the ocean increased the CH_2Br_2 sea-air flux. As anthropogenic disinfection processes in coastal areas increase, which release $CHBr_3$ and ocean warming and deoxygenation lead to more heterotrophy,[87] which may produce more CH_2Br_2, both individual sources could supply higher fractions of stratospheric bromine in the future, with yet unknown consequences for stratospheric ozone.

Increased atmospheric halocarbon concentrations can be transported from source regions in the extra tropics towards the equator by the trade winds.[6,42] Through deep convection around the equator these halocarbons are uplifted and could entrain into the stratosphere, where the bromine contributes to the

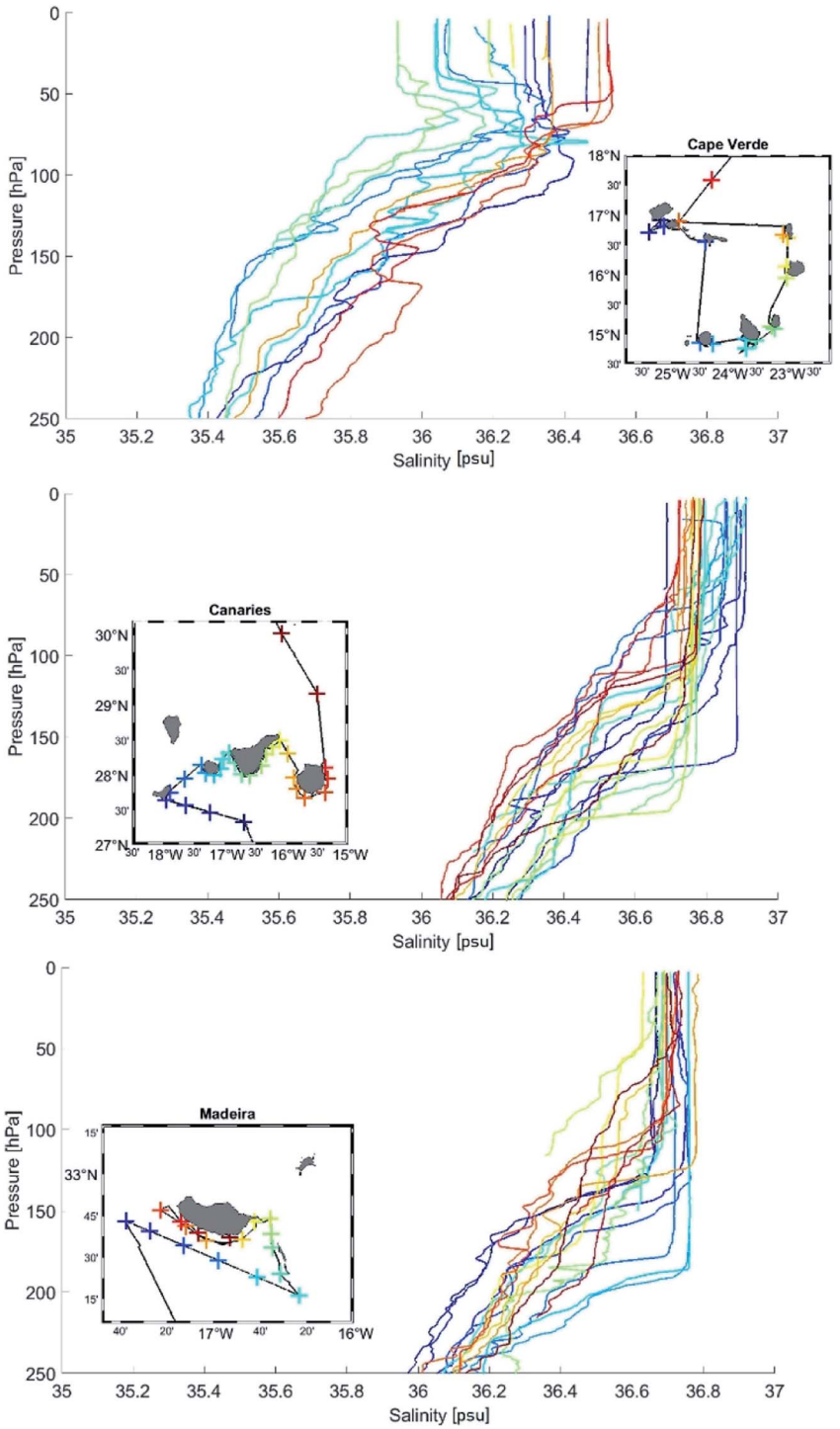

Fig. 17 Salinity profiles, color coding corresponding to CTD sampling locations.

depletion of ozone. Current modelling efforts to understand the anthropogenic signal and the sources of marine halocarbon emissions and their impact on tropospheric oxidation and stratospheric ozone and to model their future development, can benefit significantly from the findings of POS533. The region around the Macaronesian Archipelagos offers a great potential as exemplary regime to infer information for the anthropogenic interaction with marine biogeochemical cycles in order to improve the global assessments.

Appendix

The upper ocean (0–250 m)

Salinity. Northern Cape Verde Islands (red lines) displayed higher salinities (~35.6 to 36.5 psu) than the southern and southeastern stations (green lines, ~35.4 to 35.9 psu), resulting in an increasing salinity gradient with latitude. The upwelling of cold and saline water at the West African coast influenced both surface salinity and temperature at Cape Verde (Fig. 17, top). The northern islands are closer to the upwelling location and therefore displayed a stronger impact of such cold and saline water.

At the Canaries (Fig. 17, middle), where the islands were distributed mostly zonally, a salinity decrease from west (dark blue lines, ~36.2 to 36.9 psu) to east (red lines, ~36.1 to 36.7 psu) was identified. Together with the interplay of upwelling and evaporation around the western Canary Islands the intrusion of Mediterranean water leads to more saline surface waters in the west than in the east.

Salinities measured at the far eastern tip of the cruise track had the highest salinities, reaching up to 36.8 psu.

Canary Islands and Madeira upper ocean salinities were higher than Cape Verde salinities due to the impact of salty Mediterranean water around the Canaries and Madeira, but also due to high evaporation and lower rainfall than at Cape Verde.

Oxygen. The tropical NEA is known for its hyperoxic OMZ, found around the Cape Verde islands (Fig. 19, top figures). Oxygen minima of around 40 μmol kg^{-1} were discovered at Santo Antao and Sao Vicente (dark blue line). Minima reaching down to 50 μmol kg^{-1} were seen both in the north (red lines) and the south (green and turquoise lines) of the Cape Verde Islands. These minima were located between 300 m and 400 m depth. Maximum dissolved oxygen was found at the surface, where the atmosphere acts as a continuous oxygen supplier. At the bottom, oxygen was also at its maximum as AABW and other deep water masses supply oxygen upon their movement through the ocean depths.

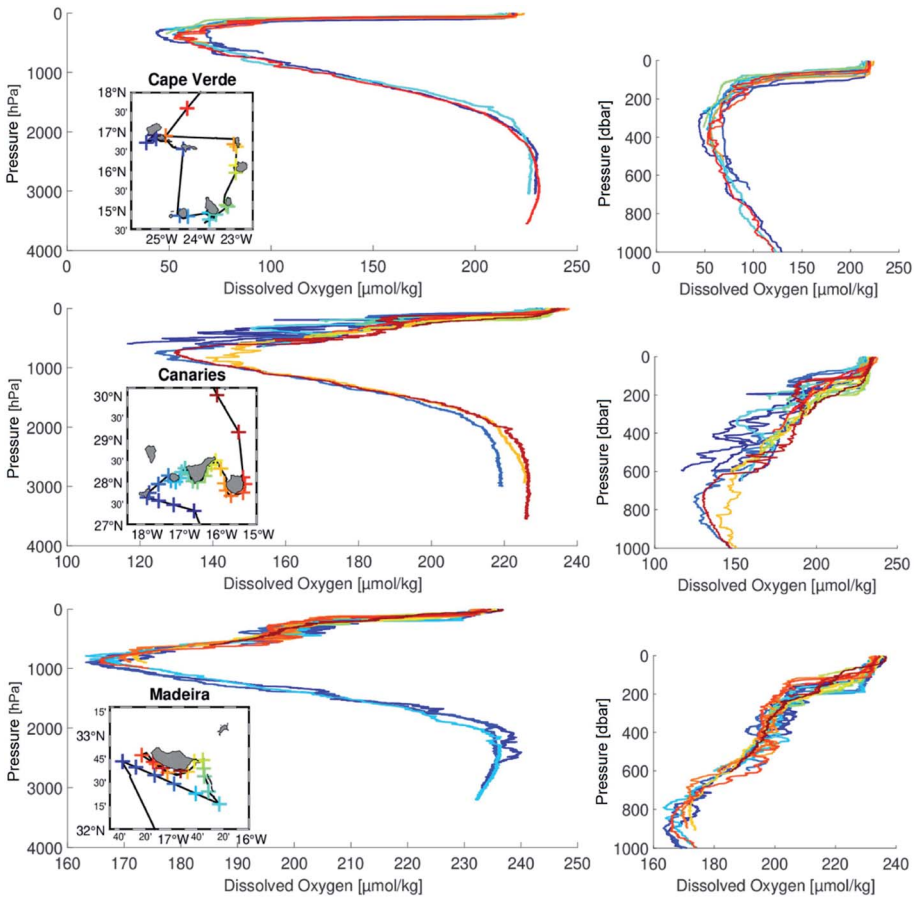

Fig. 18 Dissolved oxygen profiles, colour coding corresponding to CTD sampling location. Right graphics are full depth profiles, left graphics are surface to 1000 m depth profiles. *X*-axes are not consistent for all island groups as they vary too much for a consistent axis scale.

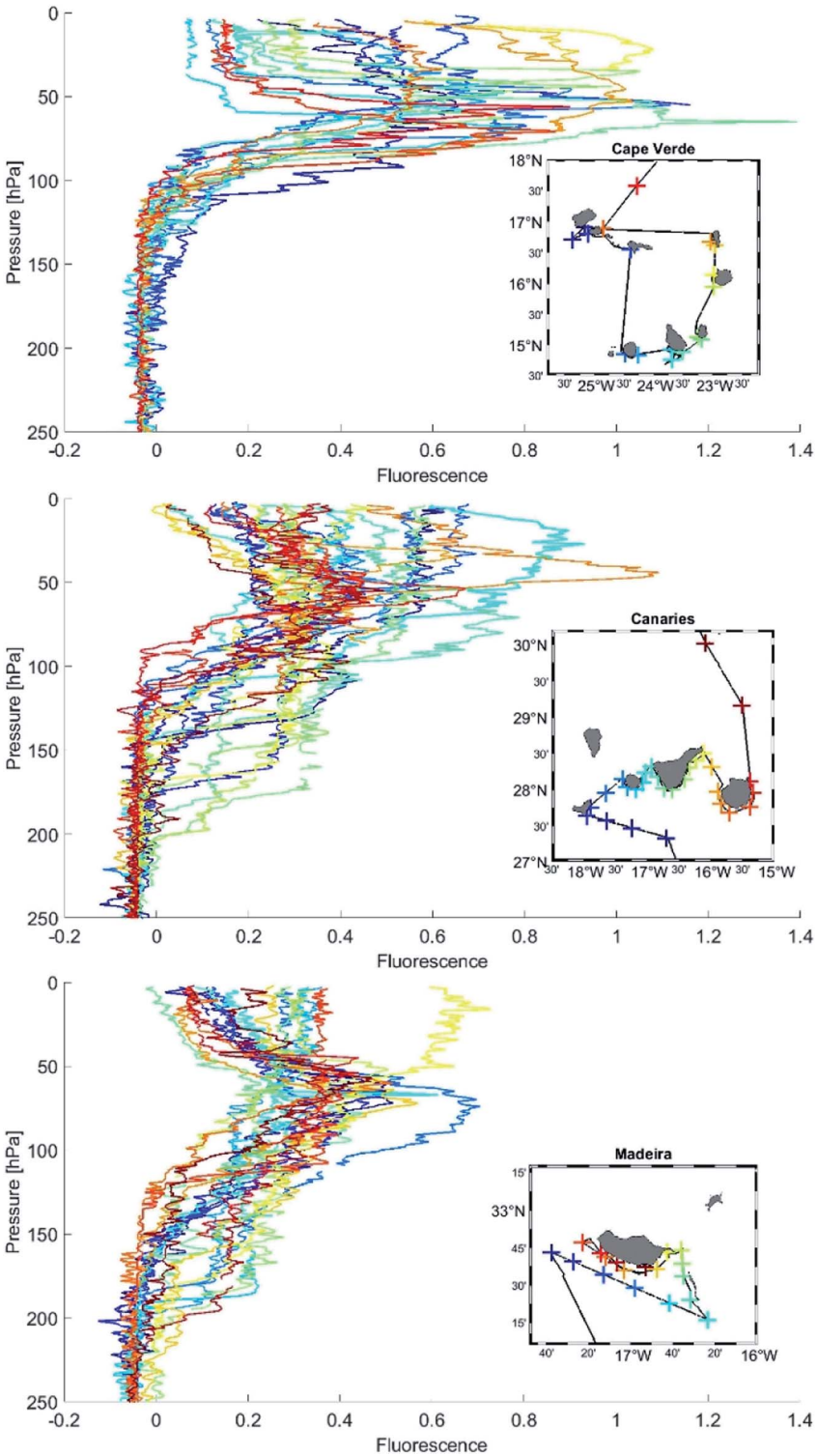

Fig. 19 Fluorescence profiles, color coding corresponding to CTD sampling location.

At the Canaries, oxygen minima were between 115 μmol kg^{-1} and 145 μmol kg^{-1} (Fig. 19, middle), and therefore is not be identified as OMZ. CTD stations taken in the south of the Canaries (dark blue lines) contained slightly less dissolved oxygen, than those in the eastern part of the islands (red lines). Karstensen *et al.*[56] also found a latitudinal dissolved oxygen gradient with decreasing oxygen values towards the equator. Causes for this gradient include ocean ventilation/transport and biogeochemical cycles. Only three profiles were taken deep enough to exhibit a water column oxygen minimum. These profiles were located between El Hierro and La Gomera (blue line), east of Tenerife (yellow line) and far north of Tenerife

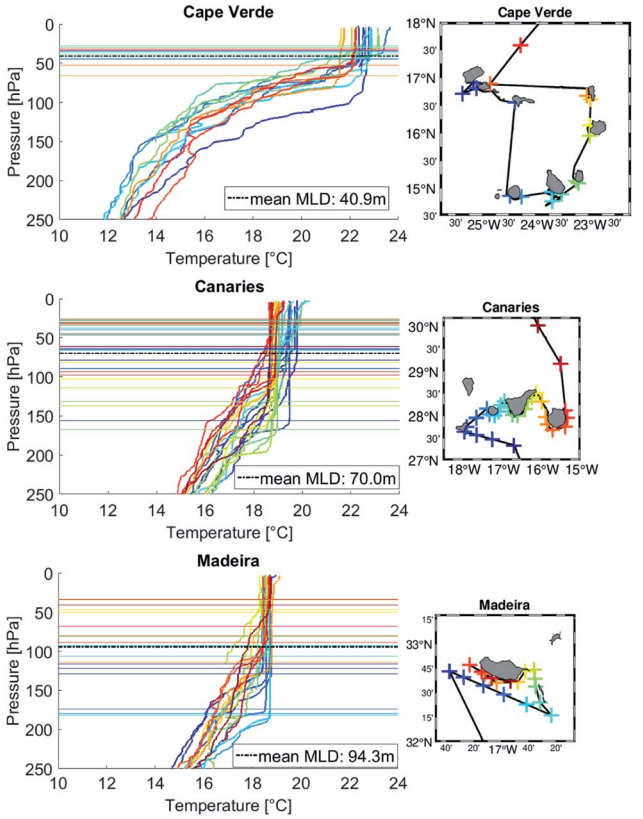

Fig. 20 Temperature profiles, color-coding corresponding to CTD sampling location. MLD for each station in equivalent color, method by Lorbacher *et al.*[89] Dotted black line: mean MLD for island group.

(dark red line) with dissolved oxygen minima at around 700–900 m depth where MW was present. The annual dissolved oxygen minimum is located at around 800 m depth, with 135–180 µmol kg^{-1} in the area around the Canaries.[56] Surface maxima were higher than at Cape Verde, reaching up to 240 µmol kg^{-1} due to the lower water temperatures, which dissolve more oxygen. At the bottom, oxygen maxima were 220–230 µmol kg^{-1} at the Canaries.

Dissolved oxygen profiles taken near Madeira did not exhibit any OMZ as the lowest values reached from 160 to 170 µmol kg^{-1} (Fig. 19, bottom). The minima were located even farther down in the water column between 800 m and 1000 m depth at the location of MW.

Fluorescence. At Cape Verde, fluorescence reached zero at around 100–150 m depth (Fig. 18, top). For stations located in the northeast (red-orange lines) fluorescence was already gone at depths of 100–120 m, whereas samples from the western Cape Verde Islands (blue lines) held fluorescence until a depth of 150 m. Enhanced local upwelling may be a cause of elevated fluorescence in the west. The effect of Mauritanian upwelling was visible, as Cape Verde fluorescence was on average higher than at the Canary Islands and Madeira data. Fluorescence maxima at Cape Verde were spread between 0.6 and 1.4. The profiles differ significantly from each other. Measurements around Sal displayed a thick fluorescence maximum (orange line), whereas the profile taken at Maio showed a distinct thin maximum. Fluorescence maxima at Boa Vista were shallow with only 30 m depth (yellow lines). Surface fluorescence was locally different, with values reaching from 0.1 in the south of Santiago (light blue line), to 0.7 at Sao Nicolau (blue line). Around the Canaries, fluorescence extended further down in the water column (Fig. 18, middle). Some profiles even reached values of 0.1 at 200 m depth (light green lines). These profiles were taken around the southern and southeastern coast of Tenerife, where strong mixing due to island wind interactions induced downwelling. Deepest maxima were found at 80 m depth reaching 0.8

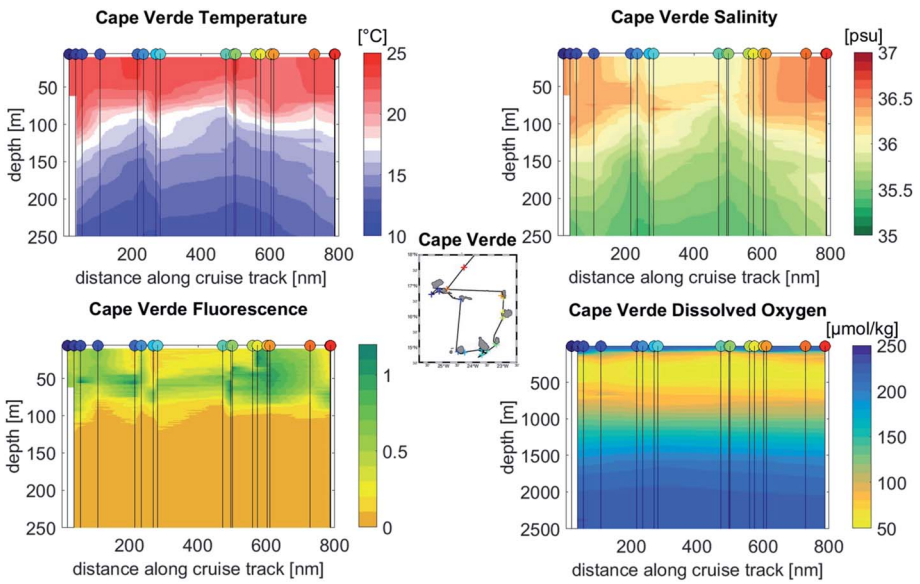

Fig. 21 Cape Verde section plots along the cruise track for different parameters. Temperature, salinity, and fluorescence were interpolated over the upper ocean (0–250 m), dissolved oxygen is shown for the ocean interior (0–2500 m). Colored circles at the top of each graphic indicate the corresponding CTD station as shown in inset map.

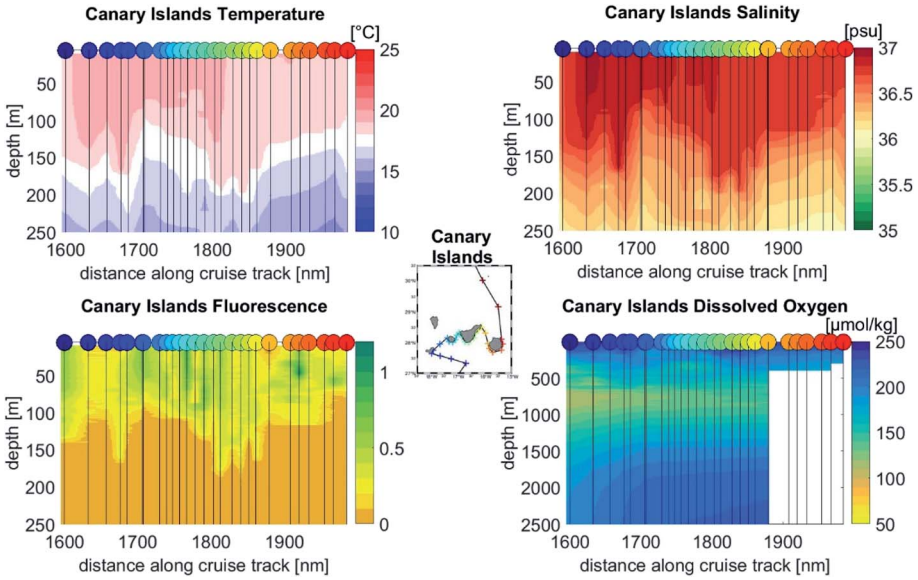

Fig. 22 Canary Islands section plots along the cruise track for different parameters. Temperature, salinity, and fluorescence were interpolated over the upper ocean (0–250 m), dissolved oxygen is shown for the ocean interior (0–2500 m). Colored circles at the top of each graphic indicate the corresponding CTD station as shown in inset map.

at the southwest of Tenerife. Profiles from Gran Canary only measured fluorescence up to a depth of around 100 m with weak maxima of approximately 0.4 at 50 m depth (red lines). However, one station off the west coast of Gran Canary displayed a fluorescence maximum of 1.1 at 50 m depth (orange line).

Similarly to the measurements taken at the Canaries, Madeira stations exhibited fluorescence even up to a depth of 200 m (Fig. 18, bottom). Most fluorescence maxima around Madeira were located at 50–60 m depth with an average of 0.5.

Mixed layer depths. Mixed layer depths (MLDs) at Cape Verde showed an overall narrow spread compared to the other islands. At Cape Verde, the deepest MLDs were found at Sal. Otherwise, most of the MLDs calculations were close to each other and could not be further assigned to a specific island. At the Canaries, maximum MLDs were essentially found around the southern to southeastern coast of Tenerife (green to yellow lines). At this location, mixing resulted from downwelling due to the island wake effect. Maximum MLDs (170–180 m) around Madeira were located at the southeastern most tip of the cruise

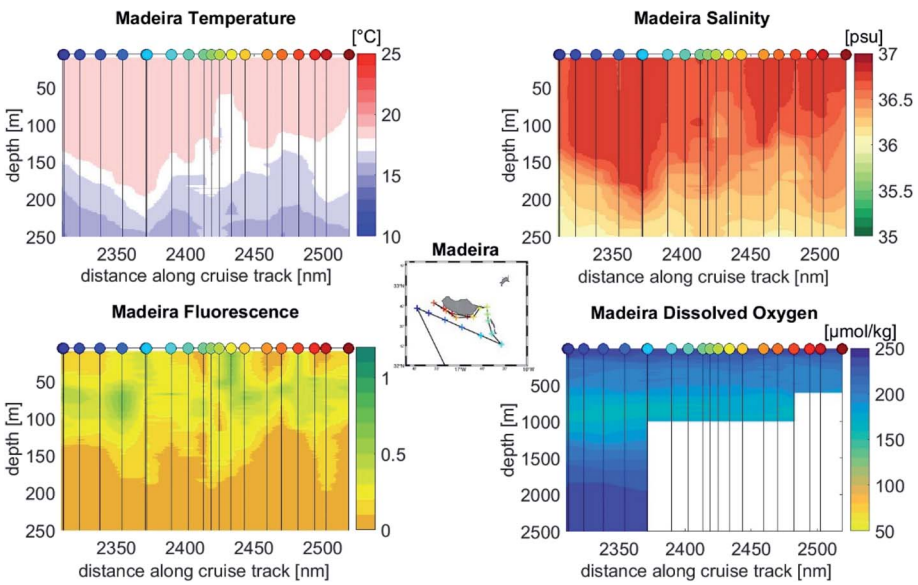

Fig. 23 Madeira section plots along the cruise track for different parameters. Temperature, salinity, and fluorescence were interpolated over the upper ocean (0–250 m), dissolved oxygen is shown for the ocean interior (0–2500 m). Colored circles at the top of each graphic indicate the corresponding CTD station as shown in inset map.

track (light blue lines). Northwest of these, medium MLDs (120–130 m) were found (dark blue lines), whereas CTDs operated closest to the island had medium to shallow MLDs (30–120 m). Especially at the eastern tip of Madeira, minimum MLDs of around 50 m (yellow lines) resulted from the swell at this location. Mean MLDs were consistent with those found in the literature.[21,88]

The upper ocean (0–250 m): an overview of the water constituents for each island group

For an overview of the most important features of the upper ocean composition, section plots give the distribution of previously discussed parameters for a better perspective (Fig. 20–22). For this the data were interpolated between stations. Dissolved oxygen figures show the upper ocean including the interior (0–2500 m), due to the OMZ at Cape Verde and other parameters are displayed only for the upper ocean (0–250 m depth).

What separated the Cape Verde ocean composition from the Canaries and Madeira, was the well pronounced OMZ at 250–500 m (Fig. 20, bottom right). Surface temperatures were highest at Cape Verde (22–25 °C), as is common for this latitude.

The upper ocean at Cape Verde was less saline than at the Canaries and Madeira, because of the less saline South Atlantic Central Water around Cape Verde than the Eastern North Atlantic Central water at higher latitudes (Fig. 20). Around the Canaries and Madeira the influence of Mediterranean water was additionally contributing to a higher salinity than at Cape Verde. Moreover, lower rainfall combined with strong evaporation are factors that are known to increase salinity at the latitudes of the Canaries and Madeira. The fluorescence maximum at Cape Verde was located at around 50 m and was strongest around the islands of Boa Vista and Sal. At Sal high fluorescence started at the surface and reached about 50 m depth.

At the Canaries, dissolved oxygen levels were a little lower at 600–1000 m depth around El Hierro, La Gomera, and Tenerife, slightly increasing from the west to the east (Fig. 21). Interior ocean dissolved oxygen at Gran Canary was not measured, as measurements were taken in shallow waters only. Surface temperatures at 0–100 m depth were on average 1.0 °C warmer at the western Islands (El Hierro, La Gomera, and western Tenerife), than at the East coast of Tenerife and Gran Canary. This pattern was similar to previously described dissolved oxygen distribution and the same profile could also be seen in the salinity, as most saline water was found in the west. Fluorescence around the Canaries was on average weaker than at Cape Verde, but stronger than at Madeira. Highest abundances were found at around 50 m, with a local maximum at the southeast of Gran Canary.

Madeira's upper ocean salinity was high (36.8 psu) to a depth of 50–100 m. At the Desertas Islands (light blue to greenish crosses) and the eastern most tip of Madeira, the surface waters were a little less saline with on average 36.6 psu. The surface temperature (50–100 m) was 18.0 °C. At the Desertas Islands and the eastern tip of Madeira, this 18.0 °C water only extended down to about 50 m depth, after which it decreased with depth. 18.0 °C water is often defined as Madeira Mode Water, in this case it was MMW (Fig. 23). Fluorescence was weaker and deeper in the waters around Madeira compared to the other island groups.

Conflicts of interest

■■■■

Acknowledgements

We thank the Review Panel German Research Vessels (Gutachterpanel Forschungsschiffe, GPF) for granting the ships time for POS533. We thank the GEOMAR for partial funding of the research cruise (Grant: EP533). Many thanks to Captain Günther and his crew, who have responded courteously to our requests and supported our shared travel success, as well as to Klas Lackschewitz for the diplomatic clearances. Many thanks to Rene Witt, Rui Salgado and Rui Caldeira for helping with the set up and equipment. Also thanks to the technical staff of the Ocean Science Center Mindelo, who provided the necessary liquid nitrogen in time for the cruise. We thank Gerd Krahman for the evaluation of the CTD-profiles, Manfred Kaufmann for help with the ecosystem-description and three reviewers for their constructive criticism on the paper. This study was carried out in cooperation with the Emmy-Noethergroup AVeSH (A new threat to the stratospheric ozone layer from Anthropogenic Very Short-lived Halocarbons) funded by the Deutsche Forschungsgemeinschaft (DFG, German Research Foundation TE 1134/1). We thank the NASA UARP grant NNX17AE43G for support of the air sampling research.

References

1 *Atmospheric chemistry in a changing world*, ed. G.P. Brasseur, R.G. Prinn and A.J. Pszenny, Springer, 2003, p. 309.

2 D. Tarasick, I. E. Galbally, O. R. Cooper, M. G. Schultz, G. Ancellet, T. Leblanc, T. J. Wallington, J. Ziemke, X. Liu, M. Steinbacher, J. Staehelin, C. Vigouroux, J. W. Hannigan, O. García, G. Foret, P. Zanis, E. Weatherhead, I. Petropavlovskikh, H. Worden, M. Osman, J. Liu, K.-L. Chang, A. Gaudel, M. Lin, M. Granados-Muñoz, A. M. Thompson, S. J. Oltmans, J. Cuesta, G. Dufour, V. Thouret, B. Hassler, T. Trickl and J. L. Neu, Tropospheric Ozone Assessment Report: Tropospheric ozone from 1877 to 2016, observed levels, trends and uncertainties, *Elem. Sci. Anth.*, 2019, 7(1), 39, DOI: : 10.1525/elementa.376.

3 L. J. Carpenter, S. D. Archer and R. Beale, Ocean-atmosphere trace gas exchange, *Chem. Soc. Rev.*, 2012, **41**, 6473–6506.

4 R. Hossaini, M. P. Chipperfield, W. Feng, T. J. Breider, E. Atlas, S. A. Montzka, B. R. Miller, F. Moore and J. Elkins, The contribution of natural and anthropogenic very short-lived species to stratospheric bromine, *Atmos. Chem. Phys.*, 2012, **12**, 371–380.

5 R. Hossaini, P. K. Patra, A. A. Leeson, G. Krysztofiak, N. L. Abraham, S. J. Andrews, A. T. Archibald, J. Aschmann, E. L. Atlas, D. A. Belikov, H. Bonisch, L. J. Carpenter, S. Dhomse, M. Dorf, A. Engel, W. Feng, S. Fuhlbrugge, P. T. Griffiths, N. R. P. Harris, R. Hommel, T. Keber, K. Kruger, S. T. Lennartz, S. Maksyutov, H. Mantle, G. P. Mills, B. Miller, S. A. Montzka, F. Moore, M. A. Navarro, D. E. Oram, K. Pfeilsticker, J. A. Pyle, B. Quack, A. D. Robinson, E. Saikawa, A. Saiz-Lopez, S. Sala, B. M. Sinnhuber, S. Taguchi, S. Tegtmeier, R. T. Lidster, C. Wilson and F. Ziska, A multi-model intercomparison of halogenated very short-lived substances (TransCom-VSLS): linking oceanic emissions and tropospheric transport for a reconciled estimate of the stratospheric source gas injection of bromine, *Atmos. Chem. Phys.*, 2016, **16**, 9163–9187.

6 S. Fuhlbrügge, B. Quack, S. Tegtmeier, E. Atlas, H. Hepach, Q. Shi, S. Raimund and K. Krüger, The contribution of oceanic halocarbons to marine and free tropospheric air over the tropical West Pacific, *Atmos. Chem. Phys.*, 2016, **16**, 7569–7585.

7 S. Tegtmeier, F. Ziska, I. Pisso, B. Quack, G. J. M. Velders, X. Yang and K. Krüger, Oceanic bromoform emissions weighted by their ozone depletion potential, *Atmos. Chem. Phys.*, 2015, **15**, 13647–13663.

8 F. Ziska, B. Quack, S. Tegtmeier, I. Stemmler and K. Krüger, Future emissions of marine halogenated very-short lived substances under climate change, *J. Atmos. Chem.*, 2017, **74**, 245–260.

9 Y. K. Lim, S. M. Phang, N. A. Rahman, W. T. Sturges and G. Malin, Halocarbon emissions from marine phytoplankton and climate change, *Int. J. Environ. Sci. Technol.*, 2017, **14**, 1355–1370.

10 Q. Liang, S. E. Strahan and E. L. Fleming, Concerns for ozone recovery Climate change mitigation and compliance with the Montreal Protocol are crucial for ozone layer recovery, *Science*, 2017, **358**, 1257–1258.

11 J. Maas, S. Tegtmeier, B. Quack, A. Biastoch, J. V. Durgadoo, S. Ruhs, S. Gollasch and M. David, Simulating the spread of disinfection by-products and anthropogenic bromoform emissions from ballast water discharge in Southeast Asia, *Ocean Sci.*, 2019, **15**, 891–904.

12 Y. Jia, S. Tegtmeier, E. Atlas and B. Quack, How marine emissions of bromoform impact the remote atmosphere, *Atmos. Chem. Phys.*, 2019, **19**, 11089–11103.

13 F. Ziska, B. Quack, K. Abrahamsson, S. D. Archer, E. Atlas, T. Bell, J. H. Butler, L. J. Carpenter, C. E. Jones, N. R. P. Harris, H. Hepach, K. G. Heumann, C. Hughes, J. Kuss, K. Krüger, P. Liss, R. M. Moore, A. Orlikowska, S. Raimund, C. E. Reeves, W. Reifenhauser, A. D. Robinson, C. Schall, T. Tanhua, S. Tegtmeier, S. Turner, L. Wang, D. Wallace, J. Williams, H. Yamamoto, S. Yvon-Lewis and Y. Yokouchi, Global sea-to-air flux climatology for bromoform, dibromomethane and methyl iodide, *Atmos. Chem. Phys.*, 2013, **13**, 8915–8934.

14 R. Hossaini, M. P. Chipperfield, S. A. Montzka, A. Rap, S. Dhomse and W. Feng, Efficiency of short-lived halogens at influencing climate through depletion of stratospheric ozone, *Nat. Geosci.*, 2015, **8**, 186–190.

15 S. T. Lennartz, G. Krysztofiak, C. A. Marandino, B. M. Sinnhuber, S. Tegtmeier, F. Ziska, R. Hossaini, K. Krüger, S. A. Montzka, E. Atlas, D. E. Oram, T. Keber, H. Bönisch and B. Quack, Modelling marine emissions and atmospheric distributions of halocarbons and dimethyl sulfide: the influence of prescribed water concentration *vs.* prescribed emissions, *Atmos. Chem. Phys.*, 2015, **15**, 11753–11772.

16 I. Stemmler, I. Hense and B. Quack, Marine sources of bromoform in the global open ocean—Global patterns and emissions, *Biogeosciences*, 2015, **12**(6), 1967–1981.

17 S. Y. Wang, D. Kinnison, S. A. Montzka, E. C. Apel, R. S. Hornbrook, A. J. Hills, D. R. Blake, B. Barletta, S. Meinardi, C. Sweeney, F. Moore, M. Long, A. Saiz-Lopez, R. P. Fernandez, S. Tilmes, L. K. Emmons and J. F. Lamarque, Ocean Biogeochemistry Control on the Marine Emissions of Brominated Very Short-Lived Ozone-Depleting Substances: A Machine-Learning Approach, *J. Geophys. Res.: Atmos.*, 2019, **124**(22), 12319–12339.

18 R. Theiler, J. C. Cook and L. P. Hager, Halohydrocarbon Synthesis By Bromoperoxidase, *Science*, 1978, **202**, 1094–1096.

19 R. Roy, Short-term variability in halocarbons in relation to phytoplankton pigments in coastal waters of the central eastern Arabian Sea, *Estuarine, Coastal Shelf Sci.*, 2010, **88**, 311–321.

20 B. Quack, E. Atlas, G. Petrick and D. W. R. Wallace, Bromoform and dibromomethane above the Mauritanian upwelling: Atmospheric distributions and oceanic emissions, *J. Geophys. Res.: Atmos.*, 2007, **112**.

21 H. Hepach, B. Quack, F. Ziska, S. Fuhlbrügge, E. L. Atlas, K. Krüger, I. Peeken and D. W. R. Wallace, Drivers of diel and regional variations of halocarbon emissions from the tropical North East Atlantic, *Atmos. Chem. Phys.*, 2014, **14**, 1255–1275.

22 A. L. Webb, E. Leedham-Elvidge, C. Hughes, F. E. Hopkins, G. Malin, L. T. Bach, K. Schulz, K. Crawfurd, C. P. D. Brussaard, A. Stuhr, U. Riebesell and P. S. Liss, Effect of ocean acidification and elevated fCO_2 on trace gas production by a Baltic Sea summer phytoplankton community, *Biogeosciences*, 2016, **13**, 4595–4613.

23 L. J. Carpenter and P. S. Liss, On temperate sources of bromoform and other reactive organic bromine gases, *J. Geophys. Res.: Atmos.*, 2000, **105**, 20539–20547.

24 P. D. Nightingale, G. Malin and P. S. Liss, Production of chloroform and other low-molecular-weight halocarbons by some species of macroalgae, *Limnol. Oceanogr.*, 1995, **40**, 680–689.

25 Y. N. Liu, D. C. O. Thornton, T. Bianchi, W. A. Arnold, M. R. Shields, J. Chen and S. A. Yvon-Lewis, Dissolved Organic Matter Composition Drives the Marine Production of Brominated Very Short-Lived Substances, *Environ. Sci. Technol.*, 2015, **49**(6), 3366–3374.

26 C. Y. Lin and S. L. Manley, Bromoform production from seawater treated with bromoperoxidase, *Limnol. Oceanogr.*, 2012, **57**(6), 1857–1866.

27 B. Quack, I. Peeken, G. Petrick and K. Nachtigall, Oceanic distribution and sources of bromoform and dibromomethane in the Mauritanian upwelling, *J. Geophys. Res.: Oceans*, 2007b, 112.

28 T. M. Vogel, C. S. Criddle and P. L. McCarty, Transformations of halogenated aliphatic compounds, *Environ. Sci. Technol.*, 1987, **21**, 722–736.

29 C. Hughes, M. Johnson, R. Uttig, S. Turner, A. Clarke and P. S. Liss, Microbial control of bromocarbon concentrations in coastal waters of the western Antarctic Peninsula, *Mar. Chem.*, 2013, **151**, 35–46.

30 K. Ichikawa, M. Kruihara, H. Tamegi and S. Hashimoto, Decomposition of brominated organic halogens by cultures of marine proteobacteria: *Phaebacter, Roseobacter*, and *Rhodobacter*, *Mar. Chem.*, 2015, **176**, 133–141.

31 T. Kataoka, A. Ooki and D. Nomura, Production of Dibromomethane and Changes in the Bacterial Community in Bromoform-Enriched Seawater, *Microbes Environ.*, 2019, **34**, 215–218.

32 H. A. Jenner, C. J. L. Taylor, M. van Donk and M. Khalanski, Chlorination by-products in chlorinated cooling water of some European coastal power stations, *Mar. Environ. Res.*, 1997, **43**, 279–293.

33 E. Agus, N. Voutchkov and D. L. Sedlak, Disinfection byproducts and their potential impact on the quality of water produced by desalination systems: a literature review, *Desalination*, 2009, **237**, 214–237.

34 D. Boudjellaba, J. Dron, G. Revenko, C. Demelas and J. L. Boudenne, Chlorination by-product concentration levels in seawater and fish of an industrialised bay (Gulf of Fos, France) exposed to multiple chlorinated effluents, *Sci. Total Environ.*, 2016, **541**, 391–399.

35 R. K. Padhi, M. Sowmya, A. K. Mohanty, S. N. Bramha and K. K. Satpathy, Formation and Speciation of Characteristics of Brominated Trihalomethanes in Seawater Chlorination, *Water Environ. Res.*, 2012, **84**, 2003–2009.

36 T. Manasfi, K. Lebaron, M. Verlande, J. Dron, C. Demelas, L. Vassalo, G. Revenko, E. Quivet and J. L. Boudenne, Occurrence and speciation of chlorination byproducts in marine waters and sediments of a semi-enclosed bay exposed to industrial chlorinated effluents, *Int. J. Hyg. Environ. Health*, 2018, **222**, 1–8.

37 G. R. Helz and R. Y. Hsu, Volatile Chlorocarbons And Bromocarbons In Coastal Waters, *Limnol. Oceanogr.*, 1978, **23**, 858–869.

38 J. D. Lee, G. McFiggans, J. D. Allan, A. R. Baker, S. M. Ball, A. K. Benton, L. J. Carpenter, R. Commane, B. D. Finley, M. Evans, E. Fuentes, K. Furneaux, A. Goddard, N. Good, J. F. Hamilton, D. E. Heard, H. Herrmann, A. Hollingsworth, J. R. Hopkins, T. Ingham, M. Irwin, C. E. Jones, R. L. Jones, W. C. Keene, M. J. Lawler, S. Lehmann, A. C. Lewis, M. S. Long, A. Mahajan, J. Methven, S. J. Moller, K. Muller, T. Muller, N. Niedermeier, S. O'Doherty, H. Oetjen, J. M. C. Plane, A. A. P. Pszenny, K. A. Read, A. Saiz-Lopez, E. S. Saltzman, R. Sander, R. von Glasow, L. Whalley, A. Wiedensohler and D. Young, Reactive Halogens in the Marine Boundary Layer (RHaMBLe): the tropical North Atlantic experiments, *Atmos. Chem. Phys.*, 2010, **10**, 1031–1055.

39 L. J. Carpenter, C. E. Jones, R. M. Dunk, K. E. Hornsby and J. Woeltjen, Air–sea fluxes of biogenic bromine from the tropical and North Atlantic Ocean, *Atmos. Chem. Phys.*, 2009, **9**, 1805–1816.

40 L. M. O'Brien, N. R. P. Harris, A. D. Robinson, B. Gostlow, N. Warwick, X. Yang and J. A. Pyle, Bromocarbons in the tropical marine boundary layer at the Cape Verde Observatory – measurements and modelling, *Atmos. Chem. Phys.*, 2009, **9**, 9083–9099.

41 L. J. Carpenter, D. J. Wevill, J. R. Hopkins, R. M. Dunk, C. E. Jones, K. E. Hornsby and J. B. McQuaid, Bromoform in tropical Atlantic air from 25 degrees N to 25 degrees S, *Geophys. Res. Lett.*, 2007, **34**. 8

42 S. Fuhlbrügge, K. Krüger, B. Quack, E. Atlas, H. Hepach and F. Ziska, Impact of the marine atmospheric boundary layer conditions on VSLS abundances in the eastern tropical and subtropical North Atlantic Ocean, *Atmos. Chem. Phys.*, 2013, **13**, 6345–6357.

43 T. Class and K. Ballschmiter, Chemistry of organic traces in air V. Determination of halogenated C1-C2-hydrocarbons in clean marine air and ambient continental air and rain by high-Resolution gas-chromatography using different stationary phases, *Fresenius Z. Anal. Chem.*, 1986, **325**, 1–7.

44 T. Class, R. Kohnle and K. Ballschmiter, Chemistry of organic traces in air VII: Bromo- and bromochloromethanes in air over the Atlantic Ocean, *Chemosphere*, 1986, **15**, 429–436.

45 T. Class and K. Ballschmiter, Chemistry of organic traces in air, VIII: sources and distribution of bromo- and bromochloromethanes in marine air and surface water of the Atlantic Ocean, *J. Atmos. Chem.*, 1988, **6**, 35–46.

46 H. Frank, W. Frank and H. J. C. Neves, Airborne C-1-halocarbons and C2-halocarbons at 4 representative sites in Europe, *Atmos. Environ., Part A*, 1991, **25**, 257–261.

47 R. G. Fischer, J. Kastler and K. Ballschmiter, Levels and pattern of alkyl nitrates, multifunctional alkyl nitrates, and halocarbons in the air over the Atlantic Ocean, *J. Geophys. Res.: Atmos.*, 2000, **105**, 14473–14494.

48 A. Ekdahl, M. Pedersen and K. Abrahamsson, A study of the diurnal variation of biogenic volatile halocarbons, *Mar. Chem.*, 1998, **63**, 1–8.

49 B. Quack, unpublished data, 2017. 9

50 P. D. Nightingale, G. Malin, C. S. Law, A. J. Watson, P. S. Liss, M. I. Liddicoat, J. Boutin and R. C. Upstill-Goddard, In situ evaluation of air–sea gas exchange parameterizations using novel conservative and volatile tracers, *Global Biogeochem. Cycles*, 2000, **14**, 373–387.

51 B. Quack and D. W. R. Wallace, Air-sea flux of bromoform: Controls, rates, and implications, *Global Biogeochem. Cycles*, 2003, **17**(1), 1023, DOI: 10.1029/2002GB001890.

52 W. J. Emery, Ocean circulation – Water Types and Water Masses, in *Encyclopedia of Atmospheric Sciences*, 2003, pp. 1556–1567.

53 M. Pastor, Meridional changes in water mass distributions of NW Africa during November 2007/2008, *Cienc. Mar.*, 2012, **38**(1B), 223–244.

54 G. Siedler, A. Kuhl and W. Zenk, The Madeira Mode Water, *J.Phys. Oceanogr.*, 1987, **17**, 1561–1570.

55 L. Stramma, P. Brandt, J. Schafstall, F. Schott, J. Fischer and A. Körtzinger, Oxygen minimum zone in the North Atlantic south and east of the Cape Verde Islands, *J. Geophys. Res.: Oceans*, 2008, **113**.

56 J. Karstensen, L. Stramma and M. Visbeck, Oxygen minimum zones in the eastern tropical Atlantic and Pacific oceans, *Prog. Oceanogr.*, 2008, **77**, 331–350.

57 E. D. Barton, J. Aristegui, P. Tett and E. N. Perez, Variability in the Canary Islands area of filament-eddy exchanges, *Prog. Oceanogr.*, 2004, **62**, 71–94.

58 J. Aristegui, E. D. Barton, X. A. Alvarez-Salgado, A. M. P. Santos, F. G. Figueiras, S. Kifani, S. Hernandez-Leon, E. Mason, E. Machu and H. Demarcq, Sub-regional ecosystem variability in the Canary Current upwelling, *Prog. Oceanogr.*, 2009, **83**, 33–48.

59 P. Sangra, A. Pascual, A. Rodriguez-Santana, F. Machin, E. Mason, J. C. McWilliams, J. L. Pelegri, C. M. Dong, A. Rubio, J. Aristegui, A. Marrero-Diaz, A. Hernandez-Guerra, A. Martinez-Marrero and M. Auladell, The Canary Eddy Corridor: A major pathway for long-lived eddies in the subtropical North Atlantic, *Deep Sea Res., Part I*, 2009, **56**, 2100–2114.

60 F. Baltar, J. Aristegui, J. M. Gasol, I. Lekunberri and G. J. Herndl, Mesoscale eddies: hotspots of prokaryotic activity and differential community structure in the ocean, *ISME J.*, 2010, **4**, 975–988.

61 R. M. A. Caldeira, A. Stegner, X. Couvelard, I. B. Araujo, P. Testor and A. Lorenzo, Evolution of an oceanic anticyclone in the lee of Madeira Island: *In situ* and remote sensing survey, *J. Geophys. Res.: Oceans*, 2014, **119**, 1195–1216.

62 J. M. Baldasano and J. Massague, Trends and patterns of air quality in Santa Cruz de Tenerife (Canary Islands) in the period 2011–2015, *Air Qual., Atmos. Health*, 2017, **10**, 939–954.

63 V. Grubisic, J. Sachsperger and R. M. A. Caldeira, Atmospheric Wake of Madeira: First Aerial Observations and Numerical Simulations, *J. Atmos. Sci.*, 2015, **72**, 4755–4776.

64 J. Pullen, R. Caldeira, J. D. Doyle, P. May and R. Tome, Modeling the air–sea feedback system of Madeira Island, *J. Adv. Model. Earth Syst.*, 2017, **9**, 1641–1664.

65 S. P. Xie, W. T. Liu, Q. Liu and M. Nonaka, Far-reaching effects of the Hawaiian Islands on the Pacific Ocean-atmosphere system, *Science*, 2001, **292**(5524), 2057–2060.

66 L. J. Carpenter, Z. L. Fleming, K. A. Read, J. D. Lee, S. J. Moller, J. R. Hopkins, R. M. Purvis, A. C. Lewis, K. Muller, B. Heinold, H. Herrmann, K. W. Fomba, D. van Pinxteren, C. Muller, I. Tegen, A. Wiedensohler, T. Muller, N. Niedermeier, E. P. Achterberg, M. D. Patey, E. A. Kozlova, M. Heimann, D. E. Heard, J. M. C. Plane, A. Mahajan, H. Oetjen, T. Ingham, D. Stone, L. K. Whalley, M. J. Evans, M. J. Pilling, R. J. Leigh, P. S. Monks, A. Karunaharan, S. Vaughan, S. R. Arnold, J. Tschritter, D. Pohler, U. Friess, R. Holla, L. M. Mendes, H. Lopez, B. Faria, A. J. Manning and D. W. R. Wallace, Seasonal characteristics of tropical marine boundary layer air measured at the Cape Verde Atmospheric Observatory, *J. Atmos. Chem.*, 2010, **67**, 87–140.

67 Y. Yokouchi, F. Hasebe, M. Fujiwara, H. Takashima, M. Shiotani, N. Nishi, Y. Kanaya, S. Hashimoto, P. Fraser, D. ToomSauntry, H. Mukai and Y. Nojiri, Correlations and emission ratios among bromoform, dibromochloromethane, and dibromomethane in the atmosphere, *J. Geophys. Res.*, 2005, **110**, D23309, DOI: 10.1029/2005JD006303.

68 S. Brinckmann, A. Engel, H. Bönisch, B. Quack and E. Atlas, Short-lived brominated hydrocarbons – observations in the source regions and the tropical tropopause layer, *Atmos. Chem. Phys.*, 2012, **12**, 1213–1228.

69 N. Myers, R. A. Mittermeier, C. G. Mittermeier, G. A. da Fonseca and J. Kent, Biodiversity hotspots for conservation priorities, *Nature*, 2000, **403**, 853–858.

70 R. Freitas, M. Romeiras, L. Silva, R. Cordeiro, P. Madeira, J. A. González, P. Wirtz, J. M. Falcón, A. Brito, S. R. Floeter, P. Afonso, F. Porteiro, M. A. Viera-Rodríguez, A. I. Neto, R. Haroun, J. N. M. Farminhão, A. C. Rebelo, L. Baptista, C. S. Melo, A. Martínez, J. Núñez, B. Berning, M. E. Johnson and S. P. Ávila, Restructuring of the 'Macaronesia' biogeographic unit: A marine multi-taxon biogeographical approach, *Sci. Rep.*, 2019, **9**(1), 15792, DOI: 10.1038/s41598-019-51786-6.

71 *Oceanographic and biological features in the Canary Current Large Marine Ecosystem*, ed. L. Valdés and I. Déniz-González, IOC-UNESCO, 2015, p. 383, Technical Series, No. 115.

72 C. Sangil, G. M. Martins, J. C. Hernández, F. Alves, A. I. Neto, C. Ribeiro, C. K. León, J. Canning-Clode, E. Rosas-Alquicira, J. C. Mendoza, I. Titley, F. Wallenstein, R. P. Couto and M. Kaufmann, Shallow subtidal macroalgae in the North-eastern Atlantic archipelagos (Macaronesian region): a spatial approach to community structure, *Eur. J. Phycol.*, 2018, **53**, 83–98.

73 C. L. Hernández, A. Serrano, T. García-Santamaría, C. Perales, P. Martín-Sosa,-P. P. Alayón, S. Jiménez, O. Tello, S. Lens and D. Macías, *Estrategia Marina, Demarcacion Marina Canaria, Parte IV. Descriptores des buen estado ambiental, descriptor 1: biodiversidad, evaluacion inicial y buen estado ambiental, Ministerio de Agricultura, Alimentación y Medio Ambiente,Secretaría General Técnica*, 2012, Centro de Publicaciones, p. 263.

74 Y. N. Liu, S. A. Yvon-Lewis, D. C. O. Thornton, J. H. Butler, T. S. Bianchi, L. Campbell, L. Hu and R. W. Smith, Spatial and temporal distributions of bromoform and dibromomethane in the Atlantic Ocean and their

relationship with photosynthetic biomass, *J. Geophys. Res.: Oceans*, 2013, **118**, 3950–3965.
75 B. Quack, E. Atlas, G. Petrick, V. Stroud, S. Schauffler and D. W. R. Wallace, Oceanic bromoform sources for the tropical atmosphere, *Geophys. Res. Lett.*, 2004, 31.
76 D. M. Karl, L. Beversdorf, K. M. Björkman, M. J. Church, A. Martinez and E. F. Delong, Aerobic production of methane in the sea, *Nat. Geosci.*, 2008, **1**, 473–478.
77 H. Hepach, B. Quack, S. Raimund, T. Fischer, E. L. Atlas and A. Bracher, Halocarbon emissions and sources in the equatorial Atlantic Cold Tongue, *Biogeosciences*, 2015, **12**, 6369–6387.
78 A. Karlsson, M. Theorin and K. Abrahamsson, Distribution, transport and production of volatile halocarbons in the upper waters of the ice-covered high Arctic Ocean, *Global Biogeochem. Cycles*, 2013, **27**, 1246–1261.
79 Y. N. Liu, S. A. Yvon-Lewis, L. Hu, J. E. Salisbury and J. E. O'Hern, $CHBr_3$, CH_2Br_2, and $CHClBr_2$ in U.S. coastal waters during the Gulf of Mexico and East Coast Carbon cruise, *J. Geophys. Res.: Oceans*, 2011, 116.
80 *Länderdateninfo*, https://www.laenderdaten.info/Afrika/Kap-Verde/tourismus.php, accessed February 2020.
81 *Kanarische Inseln*, https://de.wikipedia.org/wiki/Kanarische_Inseln#Tourismus, accessed January 2020.
82 *Madeira von A–Z*, https://www.madeira-a-z.com/die-insel/allgemeines/geschichte/tourismus.html, accessed January 2020.
83 J. J. Sadhwani and J. M. Veza JM, Desalination and energy consumption in Canary Islands, *Desalination*, 2008, **221**, 143–150.
84 F. J. Diaz-Perez, M. R. Pino-Otin, A. G. Mouhael, R. D. Martín and D. Chinarro, Energy and Water Consumption and Carbon Footprint in Tourist Pools Supplied by Desalination Plants: Case Study, the Canary Islands, *IEEE Access*, 2018, **6**, 1727–11737.
85 S. Gedik and S. Mugan-Ertugral, The effects of marine tourism on water pollution, *Fresenius Environ. Bull.*, 2019, **28**, 863–866.
86 J. S. Yang, Bromoform in the effluents of a nuclear power plant: a potential tracer of coastal water masses, *Hydrobiologia*, 2001, **464**, 99–105.
87 K. F. Kvale, K. J. Meissner and D. P. Keller, Potential increasing dominance of heterotrophy in the global ocean, *Environ. Res. Lett.*, 2015, **10**.
88 C. Troupin, P. Sangra and J. Aristegui, Seasonal variability of the oceanic upper layer and its modulation of biological cycles in the Canary Island region, *J. Marine Syst.*, 2010, **80**, 172–183.
89 K. Lorbacher, D. Dommenget, P. P. Niiler and A. Kohl, Ocean mixed layer depth: A subsurface proxy of ocean-atmosphere variability, *J. Geophys. Res.: Oceans*, 2006, **111**.